

853

**ONE DIMENSIONAL HEAVY ION BEAM TRANSPORT:
ENERGY INDEPENDENT MODEL**

**A Thesis
Presented to
The Graduate College
Hampton University**

**In Partial Fulfillment
of the Requirements for the Degree
Master of Science**

**by
Hamidullah Farhat**

April 1990

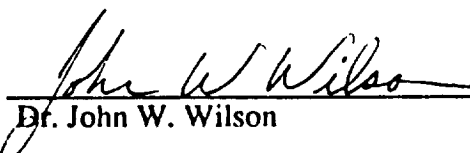
**(NASA-CR-186722) ONE DIMENSIONAL HEAVY ION
BEAM TRANSPORT: ENERGY INDEPENDENT MODEL
M.S. Thesis (Hampton Inst.) 85 p CSCL 20H**

N90-25650

**Unclass
63/72 0291069**

This thesis submitted by Hamidullah Farhat in partial fulfillment of requirements for the Degree of Master of Science in Physics at Hampton University, Hampton, Virginia, is hereby approved by the committee under whom this work has been done.


Dr. Warren W. Buck


Dr. John W. Wilson


Dr. Donald A. Whitney

Dr. Hazel J. Garrison
Assistant Vice President for Research and
Dean of the Graduate College

Date

ACKNOWLEDGEMENTS

This work was made possible by special support of some people in the Department of Physics of Hampton University and National Aeronautics and Space Administration; Langley Research Center. The work was initiated and followed by useful advice and directions of my major advisor Dr. Warren W. Buck of Hampton University and Dr. John W. Wilson from NASA Langley Research Center. They provided assistance through every phase of this work. Their generous devotion and continuous contributions to this project reflect their commitment to the advance of this field of science through research and education. Without their contributions, this work certainly would not have been possible. So, I would like to thank them so much for their cooperation. I also would like to thank all faculty members of the physics department at Hampton University for their instruction and advice and Dr. L. W. Townsend and Dr. B. M. Tabibi from NASA Langley Research Center for their advice and encouragement. I also thank my wife and daughter for their encouragement.

The present work was supported by NASA contract NAG - 1- 656 .

TABLE OF CONTENTS

	Page
ACKNOWLEDGEMENTSii
LIST OF TABLESv
LIST OF FIGURESvii
CHAPTER I. INTRODUCTION1
A. Scope of Thesis1
B. Background2
a. Radiation Sources2
Galactic Cosmic Rays3
Solar Cosmic Rays3
The Earth's Trapped Radiation4
b. Radiobiological Considerations5
c. Medical Therapy6
CHAPTER II. ONE DIMENSIONAL HEAVY ION BEAM TRANSPORT.7
A. Straight Ahead Approximation Transport Equation7
B. Energy Loss and Range- Energy Relation8
Minimum Impact Parameter12
Maximum Impact Parameter13
CHAPTER III. ENERGY INDEPENDENT HEAVY ION TRANSPORT.15
A. The Lower Limit Energy for High Energy Beam15
B. Energy Independent Flux17
C. Nuclear Absorption Cross Section18

	Page
D. Nuclear Fragmentation Parameter	19
CHAPTER IV. SOLUTIONS	20
A. Analytical Solution	20
a. Flux of Incident Ion Beam	20
b. The Flux of Secondary Fragments.	21
Flux of First Collision Term	22
Flux of Second Collision Term	22
Flux of Third Collision Term	23
Flux of Fourth Collision Term	25
B. Numerical Solution	30
CHAPTER V. APPLICATIONS	34
A. Neon Beam Transport	35
B. Iron Beam Transport	36
CHAPTER VI. SUMMARY AND CONCLUSIONS	37
REFERENCES	73

LIST OF TABLES

	Page
Table 1. The Lower Initial Energy of Incident Ions Beam to Pass the Indicated Depth of Water	39
Table 2. The Lower Initial Energy of Incident Ions Beam to Pass the Indicated Depth of Water	40
Table 3. Total Flux from Numerical Solution of Present Work Compare With Data from Reference (23)	41
Table 4. Normalized Contributions to the ^{15}O Fluxes from Successive Collision Terms of ^{20}Ne Beam Transport in Water	42
Table 5. Normalized Contribution to the ^7Li Fluxes from Successive Collision Terms of ^{20}Ne Beam Transport in Water	43
Table 6. Successive Collision Terms and the Total Fluxes of ^{18}Ne from ^{20}Ne Transport in Water	44
Table 7. Successive Collision Terms and the Total Fluxes of ^{18}F from ^{20}Ne Transport in Water	45
Table 8. Successive Collision Terms and the Total Fluxes of the ^{19}Ne from ^{20}Ne Transport in Water	46
Table 9. Successive Collision Terms and the Total Fluxes of ^{19}F from ^{20}Ne Beam Transport in Water	47
Table 10. Successive Collision Terms and the Total Fluxes of ^{10}B from ^{20}Ne Beam Transport in Water	48
Table 11. Successive Collision Terms and the Total Fluxes of ^{14}N from ^{20}Ne Beam Transport in Water	49
Table 12. Successive Collision Terms and the Total Fluxes of ^7Li from ^{20}Ne Beam Transport in Water	50
Table 13. Successive Collision Terms and the Total Fluxes of ^{12}C from ^{20}Ne Beam Transport in Water	51

	Page
Table 14. Successive Collision Terms and the Total Fluxes of ^{55}Mn from ^{56}Fe Beam Transport in Water52
Table 15. Successive Collision Terms and the Total Fluxes of ^{54}Mn from ^{56}Fe Beam Transport in Water53
Table 16. Successive Collision Terms and the Total Fluxes of ^{52}V from ^{56}Fe Beam Transport in Water54
Table 17. Successive Collision Terms and the Total Fluxes of ^{55}Fe from ^{56}Fe Beam Transport in Water55
Table 18. Normalized Contributions to the ^{52}V Fluxes from Successive Collision Terms of ^{56}Fe Beam Transport in Water56
Table 19. Normalized Contributions to the ^{16}O Fluxes from Successive Collision Terms of ^{56}Fe Beam Transport in Water.57
Table 20. Successive Collision Terms and the Total Fluxes of ^{28}Si from ^{56}Fe Beam Transport in Water58
Table 21. Successive Collision Terms and the Total Fluxes of ^{16}O from ^{56}Fe Transport in Water59

LIST OF FIGURES

	Page
Figure 1. Range-Energy Relation for Ions Lighter than ^{20}Ne with the Least Initial Energy E to Pass x Thickness of Water	60
Figure 2. Range-Energy Relation for Ions Heavier than ^{20}Ne with the Least Initial Energy E to pass x Thickness of Water	61
Figure 3. Range-Energy Relation of Incident ^{20}Ne Beam in ^{28}Si	62
Figure 4. Ratio of Calculated to Experimental Doses as a Function of Depth in Water, for a 670 MeV/nucleon ^{20}Ne Beam. The Calculation used Energy-Dependent Renormalized (VR) and Unrenormalized (ST) Silberberg-Tsao Fragmentation Parameters, and Energy-Independent Nuclear Absorption Cross section. For Reference, the Bragg Peak Location is Labeled (BP)	63
Figure 5. Ratio of Calculated to Experimental Doses, as a Function of Depth in Water, for a 670 MeV/nucleon ^{20}Ne Beam. The Calculation used Energy-Independent Renormalized (VR) Unrenormalized (ST) Silberberg-Tsao Fragmentation Parameters. The Nuclear Absorption Cross Sections were Fully Energy-Dependent. For References, the Bragg Peak Location is Labeled (BP)	64
Figure 6. Ions Fragments Flux of Various Isotopes as a Function of Depth, from ^{20}Ne Beam Transport in Water.	65
Figure 7. Flux of Some Light Ion Fragments as a Function of Depth, from ^{20}Ne Beam Transport in Water	66
Figure 8. Successive Collision Terms and the Total Fluxes of ^{18}Ne from ^{20}Ne Transport in Water	67
Figure 9. Successive Collision Terms and the Total Fluxes of ^7Li from ^{20}Ne Beam Transport in Water	68
Figure 10. Ion Fragments of Various Isotopes as a Function of Depth, from ^{56}Fe Beam Transport in Water	69

	Page
Figure 11. Total Flux of Light Ion Fragments Compared with ^{55}Fe Ion Fragments Flux, as a Function of Depth, from ^{56}Fe Transport in Water	70
Figure 12. Successive Collision Terms and the Total Fluxes of ^{52}V from ^{56}Fe Beam Transport in Water	71
Figure 13. Successive Collision Terms and the Total Fluxes of ^{54}Mn from ^{56}Fe Beam Transport in Water	72

CHAPTER I

INTRODUCTION

The interaction and propagation of high - energy heavy ions in extended matter is a subject of much current interest and activity. Transport studies are applicable to several diverse research areas including shielding against heavy ions originating from either space radiation or terrestrial accelerators, cosmic rays propagation studies in the galactic medium, or radiobiological effects resulting from workplace or clinical exposures¹. For space application, carcinogenesis or damage to nonregenerative tissues resulting from accumulated exposure to galactic heavy ions may ultimately limit an astronaut's career. In terrestrial radiation therapy and radiobiological research, knowledge of the clinical composition and interaction necessary to properly evaluate the effects on human and animal exposures dictates the need for suitable transport codes with sufficiently accurate input parameters to carry out the intended applications.

A. Scope of Thesis

In the present work, attempts to model the transport problem for heavy ion beams in various targets, employing the current level of understanding of the physics of high-charge and - energy (HZE) particle interaction with matter are made.

This work represents an energy independent transport model, with the most simplified assumptions and proper parameters. The first and essential assumption in this case (energy independent transport) is the high energy characterization of the incident beam. The energy independent equation will be solved and application will be made to

high energy neon (^{20}Ne) and iron (^{56}Fe) beams in water. The numerical solutions will be given and compared to the numerical solution of reference 23 to determine the accuracy of the model. The lower limit energy for neon and iron to be high energy beams is calculated due to Barkas and Burger theory by LBLFRG computer program developed by J. W. Wilson (NASA Langley Research Center). The calculated values in the density range of interest (50 g/cm^2) of water are: 833.43 MeV/nuc for neon and 1597.68 MeV/nuc for iron.

The analytical solutions of the energy independent transport equation gives the flux of different collision terms. The fluxes of individual collision terms are given in the tables and the total fluxes are shown in graphs relative to different thicknesses of water. The values for fluxes are calculated by the ANASTP computer code.

B. Background

It has been known for some time that there are several intense sources of radiation in space that pose a hazard to manned space flight. If man is to venture into space, adequate shielding against these radiations must be provided. To determine the shielding required, it is necessary to consider the nature and strength of the radiation, the interaction of the radiation with the shield materials, and the effect of the radiation that leaks through the shield on the astronauts². In addition, knowledge of the nature of radiation interaction with matter is necessary for radiobiological and medical therapy purposes. The detailed explanation of the indicated areas requires further special research, that is outside of the scope of this work. So each area will be discussed very briefly, only.

a. Radiation Sources

It is not necessary to give an exhaustive discussion of the radiation sources in

space. Here only the general features of the sources which are of significance to the transport problem will be discussed. There are in general, three sources of radiation in space: galactic cosmic rays, solar cosmic rays, and trapped radiation in the earth's magnetic field.

Galactic Cosmic Ray

The galactic cosmic rays are the familiar cosmic rays in the earth's atmosphere that have been studied for many years. They are composed of electrons, protons, alpha particles, antiprotons, and small admixtures of heavier elements. According to Mc Donald these cosmic rays are high energy charged particles³. The energy spectrum of these particles decreases rather rapidly with increasing energy but extends to very high energies. Fortunately the intensity of these cosmic rays is not large [≈ 2 particles/(cm² sec)] and the dose an astronaut will receive from them is of the order of 10 (rad/year) without shielding^{2, 4, 5}. This dose rate may be neglected unless very long missions are contemplated. So our consideration of these kinds of cosmic rays are very important for the career exposure of future astronauts.

Solar Cosmic Rays

Solar cosmic rays are high energy particles emitted when solar flare events take place on the sun. These particles present a major radiation hazard for space travel outside the earth's magnetic field. The particle flux is composed of protons, a varying number of alpha particles, and a small admixture of heavier nuclei² or the flux of these particles have the same composition of the galactic cosmic rays but compose the solar wind. The intensity of these particles in the vicinity of the earth builds to a maximum within the order of hours and then slowly decreases. In some cases the intensity remains above the galactic

cosmic ray background for days. During the early stages of such events, the particles angular distribution is quite anisotropic, but the distribution rather rapidly tends toward isotropy and is roughly isotropic during most of the life of the event. An extensive compilation of data on solar events may be found in the manual edited by Mc Donald⁶.

The Earth's Trapped Radiation

The trapped radiation in the earth's magnetic field, the radiation that makes up the Van Allen belts, is reasonably localized and is of primary importance. When one considers orbital missions about the earth which repeatedly pass through the belt. This radiation is mainly composed of both protons and electrons. This paper is not interested in these radiations here, but in some cases the protons are important in the transport problem for shielding purposes.

In general, the data obtained from Trans-Lunar Apollo missions show that the HZE fluence within a spacecraft in free space can be estimated at [≈ 17 particles/(cm² day)] with LET (linear energy transfer) greater than 100 KeV/mm⁷. For a theoretical three-year Mars⁸ mission during solar minimum, even behind heavy shielding, 33% of body cells would be hit by at least one particle of Z (charge number) greater than 10.

The depth-dose profiles behind the shielding materials of a spacecraft is dependent on the type, energies, and range of the primary radiation involved. Accurate transport equations and models thus depend on a knowledge of the physical interaction of HZE particles with a variety of materials over the entire range of cosmic ray energies and masses in order to provide meaningful predictions of dose distributions and other quantities required for management of space radiation hazards. Flight operational considerations impose severe constraints on shielding weight and volume limitations, and therefore is an important factor in obtaining optimal efficiency and minimal generation of secondary

radiations. Verifiable mathematical evaluations are required before innovative shielding concepts can be investigated⁹.

b. Radiobiological Considerations

When radiation (heavy ions) passes through a living cell, biological effects can be expected only when one or more ionizations occur in, or in the immediate vicinity of, some particularly radiation-sensitive molecule or structure which exists within the living cell; usually in the cell nucleus. However, ionization which occurs within the cell, but outside this volume of sensitivity is considered to be less effective. The sensitive volume is termed the "target" and the production of ionization in it is termed a "hit". The presence of the target can be demonstrated and its size and shape determined by the biological response of the organisms irradiated with a given (received) dose¹⁰.

It has been suggested that, because of the length of the track and the density of the ionization along the particle track there are important differences between the radiobiology of HZE particles and the radiobiology of other types of radiations¹¹. The relationship of relative biological effectiveness (RBE) and linear energy transfer (LET) has been determined for various end-points, but not cancer initiation. The relative biological effectiveness (RBE) cannot be determined for cases in which the end point is unique to heavy ions. Despite the problems with determination of meaningful LET values and the debate about their appropriateness, it is important to have information about the LET- RBE relationship for tumor induction, but not as important in transport problems.

There is evidence that high LET radiation at low dose rate can be more harmful than at moderately higher rates. It has been observed from energetic iron (600 MeV, 200 KeV/mm, 2 Gy/min). A similar enhancement effect has been shown for argon, but not for neon particles. Suggesting that low-dose-rate effect for cell transformation is LET

dependent, with enhancement at 140-200 KeV/mm (LBL 1988).

The combination of a complex mixture of HZE particles, energy, relative biological effectiveness with either microgravity, low LET radiations, dose protection and other factors produces great uncertainty in the ultimate level of risk and radiation protection requirements. The RBE concept is of limited use for practical applications to many radiobiological protection purposes. In radiobiological protection, many different organs, effects, dose rates and other parameters are involved and a weight factor referred to as the quality factor, (QF), is used. The QF is specified in terms of the linear collision stopping power, (S), in water, which is equal to the unrestricted linear energy transfer, LET, or LET_{α} (This is the case that locally there is no energy imparted to the medium, some times it is the same as stopping power). The relationship between QF and LET is specified by International Commission on Radiobiological Protection (ICRP 1977). Unlike RBE, QF never decreases at high LET as currently defined.

C. Medical Therapy

Heavy ions used for laboratory research are produced at particle accelerators and are generally made available in the form of a beam whose spatial extent, divergence, energy, and energy spectrum can be substantially controlled. Heavy ions were first accelerated to relativistic energies and used in radiobiological and nuclear physics experiments at the Princeton Particle Accelerator in 1971¹². The continuing heavy ion program has been the one at the Lawrence Berkeley Laboratory (LBL), where heavy ions are being studied and used for cancer therapy in order to take advantage of the steep depth-dose profiles available with accelerated beams. The heavy ion beams that have received the most interest in the biomedical program at LBL are beams of helium, carbon, neon, silicon, and argon¹³.

CHAPTER II

ONE DIMENSIONAL HEAVY ION BEAM TRANSPORT

Heavy ions, in passing through extended matter, lose their energy through interaction with atomic orbital electrons along their trajectories. On occasion there is a violent collision with nuclei of the target medium. These collisions produce projectile fragments moving in the forward direction and low-energy fragments of the struck target nucleus which are nearly isotropically distributed¹⁴.

In the present work the short-range target fragments have been neglected. The transport equation for these target fragments can be solved in closed form in terms of collision density (for more details see Wilson¹⁵). Therefore, the projectile fragment transport in the forward direction is the major subject of this work.

A. Straight Ahead Approximation Transport Equation

In this approximation, ions are not angularly deflected; and, as the colliding ions break up in nuclear fragmentation, the fragments continue in the incident ion direction. Thus, for ions of charge number j , the appropriate transport equation, neglecting target secondary fragments, is

$$\left[\frac{\partial}{\partial x} - \frac{\partial}{\partial E} \tilde{S}_j(E) + \sigma_j \right] \phi_j(x, E) = \sum_k m_{jk} \sigma_k \phi_k(x, E) \quad (2. 1)$$

where $\phi_j(x, E)$ is the flux of ions of type j with atomic mass number A_j at x in units of g/cm^2 moving along the x axis at energy E in units of MeV/nucleon; σ_j is the

corresponding macroscopic nuclear absorption cross section in unit of cm^2/g , $\tilde{\Sigma}_j(E)$ is the change in energy E per unit distance and m_{jk} is the multiplicity of ion type j produced in collision by ion type k passing the medium^{14, 16, 17}. The details for nuclear absorption cross section and multiplicities which are required for calculation in the present work, will be given in Chapter 3.

The present work is essentially concerned with high energy beams, which would not be stopped in the interested range of tissue, i.e the energy loss for them in this medium is very small or almost zero. The transport problem for such a beam is studied as an energy independent case.

B. Energy Loss and Range - Energy Relation

Charged particles such as electrons, protons, and heavy ions passing through matter, interact with nuclei and orbital electrons of the target material by the Coulombic force. For the heavy ions the two principal processes are:

1. Inelastic collisions with orbital electrons.
2. Elastic scattering from nuclei.

Other processes with much smaller cross sections include:

3. Bremsstrahlung.
4. Cerenkov Radiation.
5. Nuclear Reaction.

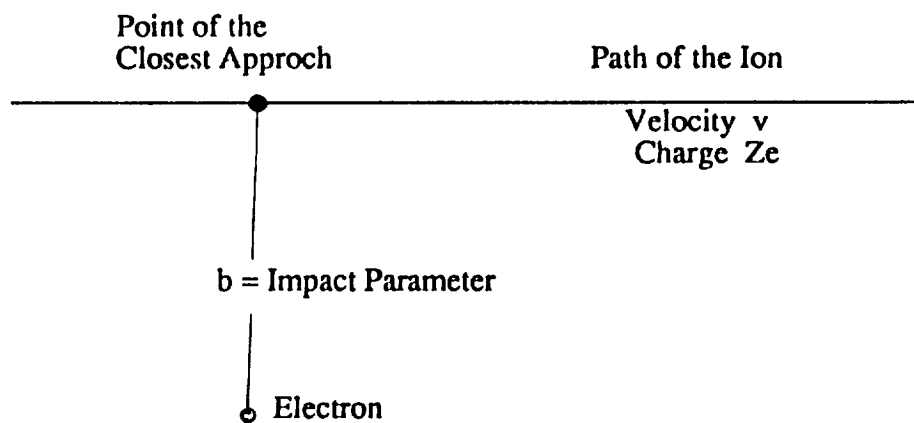
Most of the energy loss of the incident ions is a result of the inelastic collision with the orbital electrons. The energy is transferred to the target atoms causing excitation and ionization. The energy transfer per collision is very small, but a substantial energy loss is observed even in thin targets because of a large number of collisions.

There are essentially two methods of calculating the linear rate of energy loss,

or stopping power, passing through a medium. First one, based on classical considerations, was developed by Bohr (1913, 1915), and the other one is quantum mechanical method which was developed by Bethe (1930, 1933).

In classical consideration the calculation of stopping power is based on simplified assumptions concerning the structure of the material in which the ion moves. The medium is represented as an assembly of free electrons at rest and distributed uniformly in space; the charged particle is moving swiftly ($v \ll v_0$), so that the electrons do not move appreciably during a collision. Under these conditions only small momentum transfers from the ion to the electrons occur, and since the ion has a relatively large mass, its trajectory is substantially unaffected by the momentum transfers.

The collision of the moving ion with an electron is represented schematically as below;



Schematic Track of an Ion

The ion has velocity v and passes the electron at an "impact parameter" b , which is the distance of closest approach of the ion to the electron. The total momentum change of the ion from the collision with the electron is due only to the ϵ_{\perp} component of the ion's electric field.

$$\epsilon_{\perp} = \frac{Z e b}{(v^2 t^2 + b^2)^{3/2}} \quad (2. 2)$$

The momentum change, designated as ΔP_{\perp} , is given by the time integral of the force;

$$F = e \epsilon_{\perp} \quad (2. 3)$$

as

$$\Delta P_{\perp} = \int_{-\infty}^{\infty} e \epsilon_{\perp} dt = \frac{2 Z e^2 b}{v^3} \int_0^{\infty} \frac{dt}{(t^2 + b^2/v^2)^{3/2}} = \frac{2 Z e^2}{b v}. \quad (2. 4)$$

The amount of energy lost by the ion in the collision is equal to the amount of energy gained by the electron from the passage of the ion. Therefore the energy lost by the ion is given by

$$-\Delta E = \frac{(\Delta P_{\perp})^2}{2m} = \frac{2 Z^2 e^4}{m v^2 b^2}, \quad (2. 5)$$

where m is the mass of electron.

If there are n electrons per cubic centimeter, then a cylindrical section lying between impact parameters b and $(b + db)$ and having length dx , there are $2\pi n b dx$ electrons. Hence the total energy change of the ion in moving a distance dx is given by

$$dE_T = \int_{b_{\min}}^{b_{\max}} 2\pi n b (-\Delta E) db dx \quad (2. 6)$$

where b_{\min} and b_{\max} represent the "minimum" and "maximum" impact parameters, which are discussed further below. Substituting Eq. (2.5) in Eq. (2.6) and performing the integration over db , we will have

$$-\frac{dE_T}{dx} = \frac{4\pi Z^2 e^4}{mv^2} n \ln \frac{b_{\max}}{b_{\min}} . \quad (2.7)$$

The quantity $(-dE_T/dx)$ in Eq. (2.7) is known as Stopping Power, which is related to

$$\tilde{S}_j(E) = -\frac{1}{\Lambda_j} \frac{dE_T}{dx}$$

in Eq. (2.1) for ion type j .

The probability density for finding the particle at rest at a given position inside the target at a later time is known as the range distribution for the ion injected through the surface of a target. In range theory, range is regarded as the end effect of the transport problem and distributes the motion of the ion during their slowing down to zero energy.

The range of ion type j is related to stopping power $\tilde{S}_j(E)$ and depends on energy E as given by

$$R_j(E) = \int_0^E \frac{dE'}{\tilde{S}_j(E')} . \quad (2.8)$$

The stopping powers used herein are based on Ziegler's fits to a large data base¹⁸. It follows from Bethe's theory¹⁹ and classical theory (Equation 2.7) that

$$\tilde{S}_j(E) = \frac{\Lambda_P Z_j^2}{\Lambda_j Z_P^2} \tilde{S}_P(E) , \quad (2.9)$$

for which

$$\frac{Z_j^2}{\Lambda_j} R_j(E) = \frac{Z_P^2}{\Lambda_P} R_P(E) . \quad (2.10)$$

The subscript P refers to proton. Equation (2.10) is quite accurate at high energy and

only approximately true at low energies because of electron capture by the ion which effectively reduces its charge, higher order Born corrections to Bethe's theory, and nuclear stopping at the lowest energies¹⁵. Herein the parameter v_j is defined as:

$$v_j R_j(E) = v_k R_k(E) , \quad (2. 11)$$

so that

$$v_j = \frac{Z_j^2}{\Lambda_j} . \quad (2. 12)$$

Equations (2. 10) and (2. 11) are used in subsequent developments and the energy variation in v_j is neglected. The inverse function of $R_j(E)$ is defined as:

$$E = R_j^{-1} [R_j(E)] , \quad (2. 13)$$

and plays a fundamental role subsequently.

Minimum Impact Parameter

Equation (2.5) demonstrates that the energy transfer- DE is inversely proportional to the square of the impact parameter so that close collisions involve very large energy transfers. In order to apply our approximate calculations to determine b_{min} , the maximum possible energy transfer is equated to the expression (2. 5) in which we set $b = b_{min}$.

Since the velocity of the ion is considerably higher than that of the electron, it was assumed that the electron remained stationary during the collision. Following the collision, however, the electron acquires a velocity v_2 and the velocity of the ion decreases from v to v_1 . The conservation of energy for the collision can be written as :

$$\frac{1}{2} Mv^2 = \frac{1}{2} Mv_1^2 + \frac{1}{2} mv_2^2 \quad (2. 14)$$

where M is the mass of ion. For the conservation of momentum we have

$$Mv = Mv_1 + mv_2 . \quad (2. 15)$$

The maximum momentum transfer corresponds to a "head-on" collision in which the velocity vectors in Eq. (2. 15) lie in the same direction. Replacing the vectors by their magnitudes in Eq. (2. 15) and eliminating v_1 from Eqs. (2. 14) and (2. 15) we obtain for the maximum momentum transfer

$$(mv_2)_{\max} = \frac{2mM}{m+M} v . \quad (2. 16)$$

Since it is assumed that $(m/M \ll 1)$ then, approximately one can obtain

$$(mv_2)_{\max} = 2mv . \quad (2. 17)$$

The maximum energy an electron acquires as a result of a collision with an ion is

$$(DE)_{\max} = \frac{mv_2^2}{2} = 2mv^2 , \quad (2. 18)$$

which is the maximum value of the energy lost - DE by the ion. Using this expression in Eq. (2. 5), we find that the impact parameter corresponding to the maximum energy transfer is

$$b_{\min} = \frac{Ze^2}{mv^2} . \quad (2. 19)$$

Maximum Impact Parameter

For large impact parameters the duration of the collision becomes comparable with the orbital period of atomic electrons, and the electrons can no longer be treated as if they

were free. The effect of the passage of the ion on a bound electron depends on the relative collision time τ defined as

$$\tau = \frac{v}{b}, \quad (2. 20)$$

and the period of oscillation $T=2\pi/\omega$ (ω is the orbital frequency of the electron). The net transfer of momentum to an electron is most effective when $\tau \ll T$. For interaction times which are comparable to or larger than this period, the probability of a quantum transition in the atom, with an accompanying energy loss by the ion, is negligible. Thus, in order for energy to be exchanged, we have

$$\frac{b}{v} < \frac{1}{\omega}. \quad (2. 21)$$

Therefore, the maximum value of the impact parameter is given by

$$b_{\max} = \frac{v}{\omega}. \quad (2. 22)$$

CHAPTER III

ENERGY INDEPENDENT HEAVY ION TRANSPORT

If the ion beam is of sufficiently high energy (detail for high energy beam will be given in section 3. A) so that the energy shift due to atomic/molecular collisions brings none of the particles to rest in the region of interest, then we will consider a special case rather than the case where the beam lose all its energy in the medium. This case is called the energy independent case. The number of particles moving in the forward direction in the medium (apart from concerning energy) is studied as energy independent flux, which is the main subject for this work.

A. The Lower Limit Energy for High Energy Beam

According to development of technology the concept of high energy has been changed, the 3 GeV high energy particle of Bertini's time is not a high energy particle any more. Nowadays with CEBAF facilities 4 GeV particle is intermediate energy particle.

In our view point, the concept of high energy beam is not based on the technical problems. In our consideration the limit for energy is studied according to atomic/molecular interaction of the beam with the medium.

In this work, the high energy neon (^{20}Ne) and iron (^{56}Fe) beams transport in water are going to be studied. According to the theory of beam's energy loss in the medium, when a beam of ions enters a medium, its energy is lost and eventually comes to rest, after traveling a certain thickness. In the energy independent case we consider the beam of sufficient high energy that they will not come to rest in thickness L of interest.

The energy lost in crossing the thickness is less than the particle's initial energy.

$$\overline{(-\frac{dE}{dx})}L < E \quad (3. 1)$$

where $\overline{(-\frac{dE}{dx})}$ is the mean energy loss rate across the thickness L.

Now the least limit energy of the incident beam to pass through the thickness of interest is going to be studied. So for this case, it is necessary to determine the energy of the initial energy beam for the range greater than the thickness of interest, i.e, the energy of the initial beam is required for $R > L$. For this purpose we will use Equation (2. 13) will be used

$$E = R_j^{-1} [R_j(E)] \quad (2. 13)$$

To calculate the range - energy relation, subroutine RMAT has been used which is part of computer program LBLFRG developed by Wilson, J. W. (NASA Langley Research Center). These programs require a data file named ATOMICS. The calculations were done for neon and iron ion beams in water and the results are shown in Table (1) and Figure (1) for the ions lighter than neon and the results for the ions heavier than neon are shown in Table (2) and Figure (2). For evaluation of the method, the results for neon incident beam in silicon target have been compared with the results from the Handbook of Range Distributions for Energetic Ions in all Elements¹⁹ and the comparison is shown in Figure (3) .

The development of the computer codes for Range-Energy relation have been done to determine the least limit initial energy for neon and iron incident ion beams to pass 50 cm (50 g/cm²) of water, which is the maximum target thickness of interest for the purpose of Section (3. 2). From Table (1) and/or Figure (1) one can see that, the incident neon beam in water must have the initial energy greater than at least 833.43 (MeV/nuc) to

pass 50 cm of water. In the same way, from Table (2) and/or Figure (2) we can see that the incident iron beam must have the initial energy at least greater than 1579.68 (Mev/nuc) to pass 50 cm of water. So at this point the 833.43 (Mev/nuc) incident neon and 1579.68 (MeV/nuc) incident iron beams in water are the high energy beams for us.

B. Energy Independent Flux

As mentioned in Chapter 2. the energy independent flux is the main subject of present work. In this part the flux of secondary fragments from incident high energy heavy ion beams are to be studied. High energy beam means that none of the particles in the region of interest come to rest and energy loss per unit distance in the matter due to atomic/molecular collisions can be ignored in calculating the total particle flux. So that

$$\frac{dE}{dx} \equiv 0, \quad (3. 2)$$

or

$$\tilde{S}_j(E) = 0 \quad (3. 3)$$

in Equation (2. 1) and the last conclusion brings us to the energy independent case.

The energy independent transport equation is obtained from the heavy ion transport Equation (2. 1) by first assuming that the cross sections and fragmentation multiplicities are constant (independent of energy). Equation (2.1) is then integrated over all energies to yield the following energy independent transport equation.

$$\left[\frac{\partial}{\partial x} + \sigma_j \right] \phi_j(x) = \sum_k^J m_{jk} \sigma_k \phi_k(x), \quad (3. 4)$$

where $J > k > j+1$ and the initial boundary condition is

$$\phi_j(0) = \delta_{jJ}, \quad (3.5)$$

and the energy independent flux is given by

$$\phi_j(x) = \int_0^\infty \phi_j(x, E) dE. \quad (3.6)$$

The solution of Equation (3.4) for a given incident ion type j , which gives us the flux of secondary fragments, will be given in terms of g functions in Chapter (4. A).

C. Nuclear Absorption Cross-Section

Typical cosmic ray transport calculations use energy independent microscopic absorption cross sections, s_j , obtained from some form of Bradt-Peter parameterization^{21, 22}.

$$\sigma_{ij} = \pi r_0^2 \left(A_i^{\frac{1}{3}} + A_j^{\frac{1}{3}} - d \right)^2, \quad (3.7)$$

where r_0 and d are energy independent parameters which have been fitted to a particular set of cross section data and A_i and A_j are the mass numbers of colliding nuclei. While certainly adequate for high energies where the cross sections are nearly asymptotic, significant differences exist, at energies below 2 GeV/nucleon, between experimental data^{1, 21} detail of theoretical formalism and the values predicted by Equation (3.7).

To test the sensitivity of the dose predictions to the absorption cross section energy independence, the s_{ij} were fixed at their 2 GeV/nucleon values, which are representative of the asymptotic results obtained from Eq. (3.7). The input fragmentation parameters used in the calculations were the fully energy dependent ones. The results are displayed in Figure (4) as the ratios of calculated to experimental doses²⁰. For the renormalized

fragmentation parameters predictions (label VR) the calculated dose is underestimated by <10 % before the Bragg peak and up to 35 % beyond the Bragg peak. For the unrenormalized fragmentation parameters (label ST) the calculated dose is underestimated by up to 33% before the Bragg peak and by almost a factor of 4 beyond the Bragg peak.

D. Nuclear Fragmentation Parameter

Aside from the use of energy independent absorption cross section another possible simplification to the heavy ion transport problem is the use of energy independent fragmentation parameters. To test this approximation dose calculations for the neon beam in water were performed using fragmentation parameters m_{jk} fixed at the values applicable to the incident beam energy of 670 MeV/nucleon. The absorption cross sections were fully energy dependent. The results are displayed in Figure (5) as the ratios of calculated to experimental dose²⁰. For the VR fragmentation parameters, the calculated dose is within 3% of the experimental dose in the region before the Bragg peak and generally within 10% beyond the Bragg peak. For the ST fragmentation parameters, the calculated dose underestimates the experimental dose by up to 20% before the Bragg peak and by a factor of 2 beyond it. Thus, as long as fragment charge and mass are conserved through renormalization, the use of energy independent fragmentation parameters may be reasonable. Recently an energy independent fragmentation model, which conserves fragment charge and mass without renormalization, has been developed for use in heavy ion transport studies.

CHAPTER IV

SOLUTIONS

When a beam of heavy ions enters a tissue filled region, the ions break up and produce several secondary fragments. Heavy ion beams passing through tissue consist of primary particles and of fragments produced by nuclear interaction with the materials in the path of the particle beam. The produced charged fragments can include different isotopes of the primary ion and isotopes of any lighter elements, with a mass number less than the mass number of the projectile. The mathematical model for the flux of secondaries are given by the analytical solution of the Equation (3. 4).

A. Analytical Solution

Let us consider the general energy independent heavy ion beam transport equation and solve it for different collision terms :

$$\left[\frac{\partial}{\partial x} + \sigma_j \right] \phi_j(x) = \sum_k^J m_{jk} \sigma_k \phi_k(x) \quad (4. 1)$$

where the boundary condition is

$$\phi_j(0) = \delta_{jI}.$$

a. Flux of Incident Ion Beam

This part considers the portion of the incident beam which passes the target without any interaction. So, the equation for this kind of beam that is not related to any

secondary fragments is :

$$\left[\frac{\partial}{\partial x} + \sigma_j \right] \phi_j(x) = 0$$

$$\frac{\partial}{\partial x} \phi_j(x) = -\sigma_j \phi_j(x)$$

$$\frac{d\phi_j(x)}{\phi_j(x)} = -\sigma_j dx$$

$$\ln[\phi_j(x)] = -\sigma_j x + c$$

$$\phi_j(x) = e^{-\sigma_j x} e^c$$

$$x = 0 : \phi_j(0) = e^c = \delta_{jI}$$

then the flux of incident ion beam is expressed as :

$$\phi_j^{(0)}(x) = \delta_{jI} e^{-\sigma_j x} . \quad (4. 2)$$

b. The Fluxes of Secondary Fragments

To determine the fluxes of secondary fragments, the integral form of the general energy independent heavy ion beam transport of Equation (4. 1) has been considered here, which consists of the initial beam term and secondary terms as :

$$\phi_j(x) = e^{-\sigma_j x} \phi_j(0) + \sum_k \int_0^x e^{-\sigma_j z} m_{jk} \sigma_k \phi_k(x-z) dz , \quad (4. 3)$$

which is a Voltere equation, which may be solved using the Neumann series. Each term in the Neumann series is a collision term to be discussed below.

Flux of First Collision Term

In the first collision term (first generation secondaries), the first secondaries are the same as the final particles. So, subscript k can be replaced by J and there is no summation required. Then,

$$\phi_j^{(1)}(x) = \int_0^x e^{-\sigma_j z} m_{jJ} \sigma_J \phi_J(x-z) dz . \quad (4.4)$$

From equation (4.2) with

$$\phi_J(x-z) = \delta_{JJ} e^{-\sigma_J(x-z)}$$

$$\phi_J(x-z) = e^{-\sigma_J(x-z)}$$

the Equation (4.4) can be written

$$\begin{aligned} \phi_j^{(1)}(x) &= \int_0^x e^{-\sigma_j z} m_{jJ} \sigma_J e^{-\sigma_J(x-z)} dz \quad \phi_j^{(1)}(x) = \int_0^x e^{-\sigma_j z} m_{jJ} \sigma_J e^{-\sigma_J(x-z)} dz \\ &= m_{jJ} \sigma_J e^{-\sigma_J x} \int_0^x e^{(\sigma_J - \sigma_j)z} dz \\ &= m_{jJ} \sigma_J e^{-\sigma_J x} \frac{1}{\sigma_J - \sigma_j} [e^{(\sigma_J - \sigma_j)x} - 1] . \end{aligned}$$

Therefore

$$\phi_j^{(1)}(x) = \frac{m_{jJ} \sigma_J}{\sigma_J - \sigma_j} [e^{-\sigma_j x} - e^{-\sigma_J x}] . \quad (4.5)$$

Flux of Second Collision Term

In the second collision term there are secondaries from the first collision term, so the summation over k (i.e. summation over all possible types of first generation secondary

particles) is needed only. Then, the flux of second collision secondaries can be written :

$$\phi_j^{(2)}(x) = \sum_k \int_0^x e^{-\sigma_j z} m_{jk} \sigma_k \phi_k^{(1)}(x-z) dz . \quad (4.6)$$

From Equation (4. 5) replacing j by k we have :

$$\phi_k^{(1)}(x - z) = \frac{m_{kJ} \sigma_J}{\sigma_J - \sigma_k} [e^{-\sigma_k(x-z)} - e^{-\sigma_J(x-z)}]$$

and Equation (4. 6) can be written as :

$$\begin{aligned} \phi_j^{(2)}(x) &= \sum_k \int_0^x e^{-\sigma_j z} m_{jk} \sigma_k \frac{m_{kJ} \sigma_J}{\sigma_J - \sigma_k} [e^{-\sigma_k(x-z)} - e^{-\sigma_J(x-z)}] dz \\ &= \sum_k \frac{m_{jk} m_{kJ} \sigma_k \sigma_J}{\sigma_J - \sigma_k} [e^{-\sigma_k x} \int_0^x e^{(\sigma_k - \sigma_j)z} dz - e^{-\sigma_J x} \int_0^x e^{(\sigma_J - \sigma_j)z} dz] \end{aligned}$$

which reduces to

$$\phi_j^{(2)}(x) = \sum_k \frac{m_{jk} m_{kJ} \sigma_k \sigma_J}{\sigma_J - \sigma_k} \left[\frac{e^{-\sigma_j x} - e^{-\sigma_k x}}{\sigma_k - \sigma_j} - \frac{e^{-\sigma_j x} - e^{-\sigma_J x}}{\sigma_J - \sigma_j} \right] . \quad (4.7)$$

where $J-1 > k > j$ indicates all possible values of k .

Flux of Third Collision Term

In the third collision term there are secondaries from second collision term. So, the secondaries for third collision term should sum over l (i.e. summation over all possible types of second generation secondary particles). So, from equation (4. 3) the flux of third collision term secondaries is written as :

$$\phi_j^{(3)}(x) = \sum_l \int_0^x e^{-\sigma_l z} m_{jl} \sigma_l \phi_l^{(2)}(x-z) dz. \quad (4.8)$$

From Eq. (4.7) with relabeling j to l it can be written

$$\phi_l^{(2)}(x-z) = \sum_k \frac{m_{lk} m_{kl} \sigma_k \sigma_l}{\sigma_j - \sigma_k} \left[\frac{e^{-\sigma_l(x-z)} - e^{-\sigma_k(x-z)}}{\sigma_k - \sigma_l} - \frac{e^{-\sigma_l(x-z)} - e^{-\sigma_j(x-z)}}{\sigma_j - \sigma_l} \right]$$

Equation (4.8) has then the form :

$$\begin{aligned} \phi_j^{(3)}(x) &= \sum_l m_{jl} \sigma_l \int_0^x \sum_k \frac{m_{lk} m_{kl} \sigma_k \sigma_l}{\sigma_j - \sigma_k} e^{-\sigma_l z} \left[\frac{e^{-\sigma_l(x-z)} - e^{-\sigma_k(x-z)}}{\sigma_k - \sigma_l} \right. \\ &\quad \left. - \frac{e^{-\sigma_l(x-z)} - e^{-\sigma_j(x-z)}}{\sigma_j - \sigma_l} \right] dz \\ &= \sum_{lk} m_{jl} \sigma_l \frac{m_{lk} m_{kl} \sigma_k \sigma_l}{\sigma_j - \sigma_k} \int_0^x \left[\frac{e^{-\sigma_l x} e^{(\sigma_l - \sigma_k)z} - e^{-\sigma_l x} e^{(\sigma_k - \sigma_l)z}}{\sigma_k - \sigma_l} \right. \\ &\quad \left. - \frac{e^{-\sigma_l x} e^{(\sigma_l - \sigma_j)z} - e^{-\sigma_l x} e^{(\sigma_j - \sigma_l)z}}{\sigma_j - \sigma_l} \right] dz \\ &= \frac{m_{jl} m_{lk} m_{kl} \sigma_l \sigma_k \sigma_j}{\sigma_j - \sigma_k} \left[\frac{e^{-\sigma_l x}}{\sigma_k - \sigma_l} \int_0^x e^{(\sigma_l - \sigma_k)z} dz - \frac{e^{-\sigma_k x}}{\sigma_k - \sigma_l} \int_0^x e^{(\sigma_k - \sigma_l)z} dz \right. \\ &\quad \left. - \frac{e^{-\sigma_l x}}{\sigma_j - \sigma_l} \int_0^x e^{(\sigma_l - \sigma_j)z} dz + \frac{e^{-\sigma_j x}}{\sigma_j - \sigma_l} \int_0^x e^{(\sigma_j - \sigma_l)z} dz \right] \\ \phi_j^{(3)}(x) &= \sum_{lk} \frac{m_{jl} m_{lk} m_{kl} \sigma_l \sigma_k \sigma_j}{\sigma_j - \sigma_k} \left(\frac{1}{\sigma_k - \sigma_l} \left[\frac{e^{-\sigma_l x} - e^{-\sigma_k x}}{\sigma_l - \sigma_j} - \frac{e^{-\sigma_j x} - e^{-\sigma_k x}}{\sigma_k - \sigma_j} \right] \right) \end{aligned}$$

$$- \frac{1}{\sigma_J - \sigma_l} \left[\frac{e^{-\sigma_j x} - e^{-\sigma_l x}}{\sigma_l - \sigma_j} - \frac{e^{-\sigma_j x} - e^{-\sigma_J x}}{\sigma_J - \sigma_j} \right] \} . \quad (4. 9)$$

Flux of Fourth Collision Term

In the fourth collision term there are secondaries from the third collision term. So, the secondaries for fourth collision term should sum over m (i.e. summation over all possible type of third generation secondary particles).

From Equation (4. 3) the flux of fourth collision term secondaries is written :

$$\phi_j^{(4)}(x) = \sum_m \int_0^x e^{-\sigma_j z} m_{jm} \sigma_m \phi_m^{(3)}(x-z) dz , \quad (4. 10)$$

and considering Eq. (4. 9) by replacing j with m it can be written :

$$\begin{aligned} \phi_m^{(3)}(x-z) = & \sum_{lk} \frac{m_{ml} m_{lk} m_{kJ} \sigma_l \sigma_k \sigma_J}{\sigma_J - \sigma_k} \left(\frac{1}{\sigma_k - \sigma_l} \left[\frac{e^{-\sigma_m(x-z)} - e^{-\sigma_l(x-z)}}{\sigma_l - \sigma_m} \right. \right. \\ & \left. \left. - \frac{e^{-\sigma_m(x-z)} - e^{-\sigma_k(x-z)}}{\sigma_k - \sigma_m} \right] - \frac{1}{\sigma_J - \sigma_l} \left[\frac{e^{-\sigma_m(x-z)} - e^{-\sigma_l(x-z)}}{\sigma_l - \sigma_m} - \frac{e^{-\sigma_m(x-z)} - e^{-\sigma_J(x-z)}}{\sigma_J - \sigma_m} \right] \right) . \end{aligned}$$

Now Equation (4. 10) can be written :

$$\begin{aligned} \phi_j^{(4)}(x) = & \sum_m \int_0^x e^{-\sigma_j z} m_{jm} \sigma_m dz \sum_{lk} \frac{m_{ml} m_{lk} m_{kJ} \sigma_l \sigma_k \sigma_J}{\sigma_J - \sigma_k} \left(\frac{1}{\sigma_k - \sigma_l} \right. \\ & \left[\frac{e^{-\sigma_m(x-z)} - e^{-\sigma_l(x-z)}}{\sigma_l - \sigma_m} - \frac{e^{-\sigma_m(x-z)} - e^{-\sigma_k(x-z)}}{\sigma_k - \sigma_m} \right] - \frac{1}{\sigma_J - \sigma_l} \left[\frac{e^{-\sigma_m(x-z)} - e^{-\sigma_l(x-z)}}{\sigma_l - \sigma_m} \right. \\ & \left. \left. - \frac{e^{-\sigma_m(x-z)} - e^{-\sigma_J(x-z)}}{\sigma_J - \sigma_m} \right] \right) \} \end{aligned}$$

$$\begin{aligned}
\phi_j^{(4)}(x) = & \sum_{mlk} \frac{m_{jm} m_{ml} m_{lk} m_{kj} \sigma_m \sigma_l \sigma_k \sigma_j}{\sigma_j - \sigma_k} \left(\frac{1}{\sigma_k - \sigma_l} \left[\frac{1}{\sigma_l - \sigma_m} (e^{-\sigma_m x} \int_0^x e^{(\sigma_m - \sigma_l)z} dz - e^{-\sigma_l x} \int_0^x e^{(\sigma_l - \sigma_l)z} dz) - \frac{1}{\sigma_k - \sigma_m} (e^{-\sigma_m x} \int_0^x e^{(\sigma_m - \sigma_l)z} dz \right. \right. \\
& - e^{-\sigma_l x} \int_0^x e^{(\sigma_l - \sigma_l)z} dz)] - \frac{1}{\sigma_j - \sigma_l} \left[\frac{1}{\sigma_l - \sigma_m} (e^{-\sigma_m x} \int_0^x e^{(\sigma_m - \sigma_l)z} dz \right. \\
& - e^{-\sigma_l x} \int_0^x e^{(\sigma_l - \sigma_l)z} dz) - \frac{1}{\sigma_j - \sigma_m} (e^{-\sigma_m x} \int_0^x e^{(\sigma_m - \sigma_l)z} dz \\
& - e^{-\sigma_l x} \int_0^x e^{(\sigma_l - \sigma_l)z} dz)] \right) \\
\phi_j^{(4)}(x) = & \sum_{mlk} \frac{m_{jm} m_{ml} m_{lk} m_{kj} \sigma_m \sigma_l \sigma_k \sigma_j}{\sigma_j - \sigma_k} \left(\frac{1}{\sigma_k - \sigma_l} \left[\frac{1}{\sigma_l - \sigma_m} \left(\frac{e^{-\sigma_j x} - e^{-\sigma_m x}}{\sigma_m - \sigma_j} \right. \right. \right. \\
& - \frac{e^{-\sigma_j x} - e^{-\sigma_l x}}{\sigma_l - \sigma_j} \left. \right) - \frac{1}{\sigma_k - \sigma_m} \left(\frac{e^{-\sigma_j x} - e^{-\sigma_m x}}{\sigma_m - \sigma_j} - \frac{e^{-\sigma_j x} - e^{-\sigma_l x}}{\sigma_k - \sigma_j} \right)] \\
& - \frac{1}{\sigma_j - \sigma_l} \left[\frac{1}{\sigma_l - \sigma_m} \left(\frac{e^{-\sigma_j x} - e^{-\sigma_m x}}{\sigma_m - \sigma_j} - \frac{e^{-\sigma_j x} - e^{-\sigma_l x}}{\sigma_l - \sigma_j} \right) \right. \\
& \left. \left. - \frac{1}{\sigma_j - \sigma_m} \left(\frac{e^{-\sigma_j x} - e^{-\sigma_m x}}{\sigma_m - \sigma_j} - \frac{e^{-\sigma_j x} - e^{-\sigma_l x}}{\sigma_j - \sigma_j} \right) \right] \right) \quad (4.11)
\end{aligned}$$

For simplicity and easy use of these expressions for fluxes of different collision terms for computer calculations, in Equations (4.5), (4.7), (4.9), and (4.11) g-functions is introduced as follow :

1. For First Collision Term (i.e. Equation 4.5)

$$g(j,J) = \frac{e^{-\sigma_j x} - e^{-\sigma_J x}}{\sigma_J - \sigma_j} \quad (4. 12)$$

2. For Second Collision Term (i.e. Equation 4. 7)

$$g(j,k,J) = \frac{1}{\sigma_J - \sigma_k} \left[\frac{e^{-\sigma_j x} - e^{-\sigma_k x}}{\sigma_k - \sigma_j} - \frac{e^{-\sigma_j x} - e^{-\sigma_J x}}{\sigma_J - \sigma_j} \right]$$

with respect to Equation (4. 12) the last relation can be written :

$$g(j,k,J) = \frac{g(j,k) - g(j,J)}{\sigma_J - \sigma_k} . \quad (4. 13)$$

3. For Third Collision Term (i.e. Equation 4. 9)

$$\begin{aligned} g(j,l,k,J) = & \frac{1}{\sigma_J - \sigma_k} \left[\frac{1}{\sigma_k - \sigma_l} \left(\frac{e^{-\sigma_j x} - e^{-\sigma_l x}}{\sigma_l - \sigma_j} - \frac{e^{-\sigma_j x} - e^{-\sigma_k x}}{\sigma_k - \sigma_j} \right) \right. \\ & \left. - \frac{1}{\sigma_J - \sigma_l} \left(\frac{e^{-\sigma_j x} - e^{-\sigma_l x}}{\sigma_l - \sigma_j} - \frac{e^{-\sigma_j x} - e^{-\sigma_J x}}{\sigma_J - \sigma_j} \right) \right] , \end{aligned} \quad (4. 14)$$

and considering relation (4. 12), and switching the indices in Equation (4.14) it will have the form:

$$g(j,k,l,J) = \frac{1}{\sigma_J - \sigma_l} \left[\frac{g(j,k) - g(j,l)}{\sigma_l - \sigma_k} - \frac{g(j,k) - g(j,J)}{\sigma_J - \sigma_j} \right] .$$

With respect to Equation (4. 13) the last relation takes the form :

$$g(j,k,l,J) = \frac{g(j,k,l) - g(j,k,J)}{\sigma_J - \sigma_l} \quad (4. 15)$$

4. For Fourth Collision Term (i.e. Equation 4. 11)

$$\begin{aligned}
g(j,m,l,k,J) = & \frac{1}{\sigma_J - \sigma_k} \left(\frac{1}{\sigma_k - \sigma_l} \left[\frac{1}{\sigma_l - \sigma_m} \left(\frac{e^{-\sigma_j x} - e^{-\sigma_m x}}{\sigma_m - \sigma_j} - \frac{e^{-\sigma_j x} - e^{-\sigma_l x}}{\sigma_l - \sigma_j} \right) \right. \right. \\
& - \frac{1}{\sigma_k - \sigma_m} \left(\frac{e^{-\sigma_j x} - e^{-\sigma_m x}}{\sigma_m - \sigma_j} - \frac{e^{-\sigma_j x} - e^{-\sigma_k x}}{\sigma_k - \sigma_j} \right) \left. \right] - \frac{1}{\sigma_J - \sigma_l} \left[\frac{1}{\sigma_l - \sigma_m} \left(\frac{e^{-\sigma_j x} - e^{-\sigma_m x}}{\sigma_m - \sigma_j} \right. \right. \\
& \left. \left. - \frac{e^{-\sigma_j x} - e^{-\sigma_l x}}{\sigma_l - \sigma_j} - \frac{1}{\sigma_J - \sigma_m} \left(\frac{e^{-\sigma_j x} - e^{-\sigma_m x}}{\sigma_m - \sigma_j} - \frac{e^{-\sigma_j x} - e^{-\sigma_J x}}{\sigma_J - \sigma_j} \right) \right] \right) .
\end{aligned}$$

Considering equation (4. 12) and switching k with m to each other in the last relation it will have the form:

$$\begin{aligned}
g(j,k,l,m,J) = & \frac{1}{\sigma_J - \sigma_m} \left(\frac{1}{\sigma_m - \sigma_l} \left[\frac{g(j,k) - g(j,l)}{\sigma_l - \sigma_k} - \frac{g(j,k) - g(j,m)}{\sigma_m - \sigma_k} \right] \right. \\
& \left. - \frac{1}{\sigma_J - \sigma_l} \left[\frac{g(j,k) - g(j,l)}{\sigma_l - \sigma_k} - \frac{g(j,k) - g(j,J)}{\sigma_J - \sigma_k} \right] \right)
\end{aligned}$$

with regarding Equation (4. 13) it can be written:

$$\begin{aligned}
g(j,k,l,m,J) = & \frac{1}{\sigma_J - \sigma_m} \left(\frac{1}{\sigma_m - \sigma_l} [g(j,k,l) - g(j,k,m)] \right. \\
& \left. - \frac{1}{\sigma_J - \sigma_l} [g(j,k,l) - g(j,k,J)] \right) .
\end{aligned}$$

According to Equation (4. 15) the last relation will have the form :

$$g(j,k,l,m,J) = \frac{g(j,k,l,m) - g(j,k,l,J)}{\sigma_J - \sigma_m} , \quad (4. 16)$$

with considering Equations (4. 12), (4. 13), (4. 15), and (4. 16) we can write the general form for g - functions as :

$$g(j_1, j_2, j_3, \dots, j_n, j_{n+1}) = \frac{g(j_1, j_2, \dots, j_n) - g(j_1, j_2, \dots, j_{n-1}, j_{n+1})}{\sigma_{j_{n+1}} - \sigma_{j_n}} \quad (4. 17)$$

where :

$$g(j_1) = e^{-\sigma_{j_1} x} . \quad (4. 18)$$

Now by switching 1 with k in $\phi_j^{(3)}(x)$ and m with k in $\phi_j^{(4)}(x)$ according to the left sides of the Eqs. (4. 12), (4. 13), (4. 15), and (4. 16) the following very simple form for $\phi_j^{(1)}(x)$, $\phi_j^{(2)}(x)$, $\phi_j^{(3)}(x)$, $\phi_j^{(4)}(x)$ can be written:

$$\phi_j^{(1)}(x) = \sigma_{jJ} g(j,J) , \quad (4. 19a)$$

$$\phi_j^{(2)}(x) = \sum_k \sigma_{jk} \sigma_{kJ} g(j,k,J) , \quad (4. 19b)$$

$$\phi_j^{(3)}(x) = \sum_{k,l} \sigma_{jk} \sigma_{kl} \sigma_{lJ} g(j,k,l,J) , \quad (4. 19c)$$

$$\phi_j^{(4)}(x) = \sum_{k,l,m} \sigma_{jk} \sigma_{kl} \sigma_{lm} \sigma_{mJ} g(j,k,l,m,J). \quad (4. 19d)$$

where

$$m_{jJ} \sigma_J = \sigma_{jJ} ,$$

$$m_{jk} \sigma_k = \sigma_{jk} , m_{kJ} \sigma_J = \sigma_{kJ} ,$$

$$m_{jk} \sigma_k = \sigma_{jk} , m_{kl} \sigma_l = \sigma_{kl} , m_{lJ} \sigma_J = \sigma_{lJ} ,$$

$$m_{jk} \sigma_k = \sigma_{jk} , m_{kl} \sigma_l = \sigma_{kl} , m_{lm} \sigma_m = \sigma_{lm} , m_{mJ} \sigma_J = \sigma_{mJ} .$$

The total flux of secondary fragments in different thicknesses x of the target is

$$\phi_j(x) = \sum_i \phi_j^{(i)}(x) , \quad (4. 20)$$

i indicates the collision (i.e. generation) number.

The Equation (4. 20) which is the solution for energy independent transport equation, is equivalent to the one derived by Ganapol et al.²³. In this stage it is better to

study the numerical solution of the above formalism.

B. Numerical Solution

To evaluate the accuracy of the model solve Equation (4. 1) numerically. For this purpose one can start from a simple approximation of the derivatives.

$$\frac{d\bar{\phi}(x)}{dx} = \frac{\bar{\phi}(x+\Delta x) - \bar{\phi}(x)}{\Delta x}$$

with very small Δx ($\Delta x \rightarrow 0$).

$$\bar{\phi}(x+\Delta) = \bar{\phi}(x) + \frac{d\bar{\phi}(x)}{dx} \Delta + o(\Delta^2) + \dots \quad (4. 21)$$

To determine $(d\phi(x)/dx)$ let us consider the general energy independent transport equation

$$\left[\frac{\partial}{\partial x} + \sigma_j \right] \phi_j(x) = \sum_k m_{jk} \sigma_k \phi_k(x)$$

is considered and expanded for $J \geq k > j$, where J denotes the incident ion beam's charge number.

$$\left[\frac{d}{dx} + \sigma_1 \right] \phi_1(x) = 0 + m_{12}\sigma_2\phi_2(x) + m_{13}\sigma_3\phi_3(x) + \dots + m_{1J}\sigma_J\phi_J(x)$$

$$\left[\frac{d}{dx} + \sigma_2 \right] \phi_2(x) = 0 + 0 + \dots + m_{23}\sigma_3\phi_3(x) + \dots + m_{2J}\sigma_J\phi_J(x)$$

(4. 22)

$$\left[\frac{d}{dx} + \sigma_J \right] \phi_J(x) = 0 + 0 + \dots + 0$$

The system of Equations (4. 22) can be written in matrix representation as :

$$\frac{d\bar{\phi}(x)}{dx} + \bar{\sigma} \bar{\phi}(x) = \bar{A} \bar{\phi}(x)$$

or :

$$\frac{d\bar{\phi}(x)}{dx} = A \bar{\phi}(x) - \bar{\sigma} \bar{\phi}(x) . \quad (4. 23)$$

where A is the matrix of fragmentation parameters and shown as :

$$A = \begin{vmatrix} 0 & m_{12}s_2 & m_{13}s_3 & . & . & . & m_{1J}s_J \\ 0 & 0 & m_{23}s_3 & . & . & . & m_{2J}s_J \\ 0 & 0 & 0 & . & . & . & m_{3J}s_J \\ . & . & . & . & . & . & . \\ . & . & . & . & . & . & . \\ . & . & . & . & . & . & . \\ 0 & 0 & 0 & . & . & . & 0 \end{vmatrix}$$

The entries of matrix A satisfy the assumed simplified nuclear model²³. According to this model

$$m_{jk} = \begin{cases} \frac{2}{k-1} & k > j \\ 0 & k \leq j \end{cases}$$

and

$$\sigma_j = \sigma_0 j^{(2/3)}$$

Here the choice of σ_j is based upon nuclear liquid drop model, and the multiplicities are chosen so as to conserve charge in each interaction. The matrix for nuclear absorption

cross section has the form :

$$\bar{\sigma} = \begin{bmatrix} \sigma_1 & 0 & . & . & . & 0 \\ 0 & \sigma_2 & . & . & . & 0 \\ . & . & . & . & . & . \\ . & . & . & . & . & . \\ 0 & 0 & . & . & . & \sigma_J \end{bmatrix}$$

where the solution matrix is like :

$$\bar{\phi}(x) = \begin{bmatrix} \phi_1(x) \\ \phi_2(x) \\ \phi_3(x) \\ . \\ . \\ \phi_J(x) \end{bmatrix}$$

So, with the known values of A and σ in Equation (4. 23), we can easily determine the values of $f(x+D)$ from the Equation (4. 21):

$$\phi(x+\Delta) = \bar{\phi}(x) + \frac{d\bar{\phi}(x)}{dx} \Delta$$

where the initial condition is :

$$\phi(0) = \begin{bmatrix} 0 \\ 0 \\ 0 \\ . \\ . \\ 1 \end{bmatrix}$$

The results of calculation for ^{25}Mg incident beam in water in thicknesses up to 100

(g/cm²) has been done by computer code IONFLM (i.e. the program which has been developed for calculation of total flux related to Eq. 4. 21). The same calculation for ²⁵Mg was done by Ganapol et al.²³. In Table (1) the results for total flux from this code is compared with the results from reference 23.

CHAPTER V

APPLICATIONS

In this part the application of the energy independent beam transport formalism is going to be studied in order to calculate the four different contributing terms and total flux from incident neon (^{20}Ne) and iron (^{56}Fe) beams in water. The maximum depth of interest for both neon and iron cases is 50 g/cm^2 (50 cm, special for water as target). From the energy independent formalism, our incident beams must have sufficient energy to pass the range of interest (detail in previous chapters). Based on the calculations of Chapter (3. 1) the least initial energy for the neon beam must be 833.43 MeV/nuc and the iron incident beam must have 1597.68 MeV/nuc initial energy to qualify as high energy beams for our case. Using the computer programs and subroutines developed for the equations derived from the energy independent transport equation in Chapter (4.1), the different contributing terms and the total flux of different generation secondary fragments have been calculated. The related equations from Chapter (4. A) are the following :

Incident beam :

$$\phi_j^{(0)}(x) = \delta_{jJ} e^{-\sigma_j x}$$

Flux of 1st generation secondaries :

$$\phi_j^{(1)}(x) = \sigma_{jJ} g(j,J)$$

Flux of 2nd generation secondaries :

$$\phi_j^{(2)}(x) = \sum_k \sigma_{jk} \sigma_{kJ} g(j,k,J)$$

Flux of third generation secondaries :

$$\phi_j^{(3)}(x) = \sum_{k,l} \sigma_{jk} \sigma_{kl} \sigma_{lJ} g(j,k,l,J)$$

Flux of fourth generation secondaries :

$$\phi_j^{(4)}(x) = \sum_{k,l,m} \sigma_{jk} \sigma_{kl} \sigma_{lm} \sigma_{mJ} g(j,k,l,m,J)$$

The total flux for all secondary fragments :

$$\phi_j(x) = \sum_i \phi_j^{(i)}(x) \quad i = 1, 2, 3, 4$$

Now, the specific terms will be discussed.

A. Neon Beam Transport

In the case of neon (^{20}Ne) incident beam transport on water first it is noted that ^{19}Ne and ^{19}F have only one contributing term in Equation (4. 20). The fluxes of these secondary fragments and some other secondary ion fragments are shown in Figures (6), (8), (9) and Tables (6 - 10). The effect of successive terms of Equation (4. 20) is shown in Table (6) for Oxygen (^{16}O) flux. From the Table (6) it is clear that the fourth and higher order collision terms are completely negligible, and that third collision terms are rather minor contributions. The relative magnitude of the terms contributing to the ^7Li flux generated by the ^{20}Ne beam is presented in Table (7). The fourth collision term is negligible at small penetration distances and it is small, but not negligible, at distances

greater than 30 g/cm². The fluxes of secondary fragments for some lighter ions which are produced in ²⁰Ne beam transport in water are presented in Figure (7) and Tables (11 - 13).

B. Iron Beam Transport

In the case of ⁵⁶Fe incident beam on water it is noted that ⁵⁵Fe and ⁵⁵Mn have only one contributing term in Equation (4. 20). The ⁵⁴Mn has two contributing terms in Equation (4. 20), and the results can be seen in Figure (10) compared with some other ion secondary fragment fluxes. Also, the fluxes of some secondaries from ⁵⁶Fe beam include the results for ⁵²V are shown in Tables (14 - 17). The convergence rate of Eq. (4. 20) is determined in Table (18) for vanadium ⁵²V from iron ⁵⁶Fe beam on water. Again we see the fourth collision term to be negligible while the three term expansion that has been used by Wilson et al.²⁴, before seems quite accurate at these depths for these ions. In distinction to prior results, the ¹⁶O flux has significant contributions from higher order terms for depths beyond 20 g/cm² as seen in Table (19). Also, the fluxes of secondary fragments for some lighter ions compare with ⁵⁵Fe which are produced in ⁵⁶Fe beam transport in water, are presented in Figure (11) and Tables (17) (20), (21). Figures (12) and (13) show the comparison of the total flux and the fluxes of individual collision terms.

CHAPTER VI

SUMMARY AND CONCLUSIONS

Determination of the fluxes of secondary fragments in an energy independent model of heavy ions beam transport in one dimension is the focal point of this work. The concept of energy independent term is related to high energy incident beam in a medium which passes the interested thickness of the medium without coming to rest. The solutions which give the fluxes of secondary fragments for different generations, are obtained from the integral form of the energy independent transport equation analytically. The numerical solution of the general energy independent transport equation gives us the results for total flux of secondary fragments of all generations. The results are compared to benchmark results of reference 23 in order to determine the accuracy of the model.

The fluxes of secondary fragments of incident ^{20}Ne beam with initial energy 833.43 MeV/nuc and incident iron ^{56}Fe beam with the initial energy 1597.68 MeV/nuc has been studied in 50 g/cm² of water (which almost represents normal tissue). Results show that fourth and higher order collision terms are negligible, and third collision terms are rather minor. Also it is seen that with exceptions of the lighter isotopes of the primary ions secondary ions are exponentially attenuated at a slower rate than the primaries.

The calculations in this present method have taken a rather long execution time on computer. The next step of this work will be the studying of the same model with a different method which is expected to take less computer execution time.

A rather important thing for transport problems of this kind is the solution of

coupled partial differential equations which requires a special work. As has been indicated in reference 23, the solution of this kind of equation for transport problem will be the subject of their future work²³.

Table 1
The Lower Initial Energy of Incident Ions Beam to Pass
the Indicated Depth of Water

Depth (g/cm ²)	Incident Ions with Initial Energy (MeV/nucleon)				
	¹⁶ O	¹² C	¹⁹ F	⁴ He	¹⁰ B
5.000	172.494	146.320	178.920	78.772	131.934
10.000	258.959	218.441	268.944	116.180	196.344
15.000	330.383	277.918	343.416	146.413	249.223
20.000	394.362	330.482	410.416	172.567	296.107
25.000	454.171	378.968	473.026	196.344	338.870
30.000	510.431	424.845	531.644	218.435	379.088
35.000	563.695	468.560	587.689	239.234	417.388
40.000	615.369	510.425	641.916	258.990	454.254
45.000	665.693	550.507	694.752	277.907	489.708
50.000	714.815	589.713	746.549	296.107	524.017
55.000	762.964	628.092	797.186	313.587	557.105
60.000	810.134	665.834	846.589	330.550	589.713
65.000	856.280	702.794	895.457	347.092	621.748
70.000	902.059	739.106	943.888	363.258	653.360
75.000	947.460	774.866	991.941	379.088	684.398
80.000	992.532	810.127	1039.468	394.613	714.969
85.000	1037.133	844.770	1086.528	409.861	745.103
90.000	1081.320	879.220	1133.190	424.888	774.866
95.000	1125.152	913.442	1179.489	439.657	804.283
100.000	1162.660	947.460	1225.459	454.203	833.379

Table 2
The Lower Initial Energy of Incident Ions Beam to Pass
the Indicated Depth of Water

Depth (g/cm ²)	Incident Ions with Initial Energy (MeV/nucleon)				
	²⁰ Ne	⁵⁶ Fe	⁵⁵ Mn	⁵⁹ Co	¹⁰⁶ Pd
5.000	196.226	330.692	318.825	335.360	450.698
10.000	295.929	511.434	491.972	519.119	711.602
15.000	378.825	667.791	641.335	678.260	943.639
20.000	454.171	812.888	779.701	826.089	1163.337
25.000	524.039	950.582	910.493	966.638	1376.136
30.000	589.736	1085.420	1038.463	1104.218	1586.473
35.000	652.985	1216.657	1163.080	1238.116	1794.732
40.000	714.507	1343.935	1285.140	1368.056	2001.386
45.000	774.791	1471.377	1404.273	1498.267	2207.027
50.000	833.431	1597.681	1523.776	1627.328	2411.891
55.000	890.651	1723.230	1642.327	1755.684	2616.257
60.000	947.461	1848.237	1760.331	1883.514	2819.421
65.000	1003.740	1972.841	1877.896	2010.955	3024.518
70.000	1059.273	2097.151	1995.128	2137.891	3230.909
75.000	1114.225	2220.975	2111.916	2264.811	3438.660
80.000	1168.660	2344.982	2228.645	2391.757	3650.336
85.000	1222.630	2469.049	2345.382	2518.785	3859.751
90.000	1276.182	2593.221	2462.172	2645.940	4069.704
95.000	1328.465	2717.537	2579.054	2773.261	4279.159
100.000	1381.473	2842.085	2696.059	2900.820	4490.042

Table 3
Total Flux from Numerical Solution of Present Work Compare
with Data from Reference 23

Depth (g /cm ²)	Total Flux (Ions/cm ²)	
	Present Work	Data from Ref. 23
0.000	1.000	1.000
10.000	2.150	2.159
20.000	3.438	3.452
30.000	4.793	4.801
40.000	6.124	6.137
50.000	7.396	7.401
60.000	8.532	8.547
70.000	9.541	9.543
80.000	10.359	10.363
90.000	10.996	11.011
100.000	11.465	11.473

Table 4

Normalized Contributions to the ^{15}O Fluxes from Successive
Collision Terms of ^{20}Ne Beam Transport in Water

Depth (g/cm ²)	Fluxes of Different Collision Terms in (Ions/cm ²)			
	First Term	Second Term	Third Term	Forth Term
5.000	1.00E 0	5.03E-2	6.58E-4	3.63E-6
10.000	1.00E 0	1.01E-1	2.63E-3	3.31E-5
20.000	1.00E 0	1.05E-1	5.91E-3	1.07E-5
25.000	1.00E 0	2.01E-1	1.05E-2	2.57E-4
30.000	1.00E 0	2.52E-1	1.64E-2	4.92E-4
35.000	1.00E 0	3.02E-1	2.36E-2	8.58E-4
40.000	1.00E 0	3.53E-1	3.21E-2	1.36E-3
45.000	1.00E 0	4.03E-1	4.18E-2	2.03E-3
50.000	1.00E 0	5.04E-1	6.52E-2	3.95E-3

Table 5

Normalized Contributions to the ^7Li Fluxes from Successive
Collision Terms of ^{20}Ne Beam Transport in Water

Depth (g/cm ²)	Fluxes of Different Collision Terms in (Ions/cm ²)			
	First Term	Second Term	Third Term	Forth Term
5.000	1.00E 0	2.18E-2	2.91E-3	
10.000	1.00E 0	1.62E-1	1.15E-2	4.02E-4
15.000	1.00E 0	2.42E-1	2.57E-2	
20.000	1.00E 0	3.20E-1	4.53E-2	3.16E-3
25.000	1.00E 0	3.97E-1	7.01E-2	
30.000	1.00E 0	4.72E-1	9.98E-2	1.04E-2
35.000	1.00E 0	5.46E-1	1.34E-1	
40.000	1.00E 0	6.18E-1	1.73E-1	2.39E-2
50.000	1.00E 0	7.58E-1	2.63E-1	4.53E-2

Table 6
Successive Collision Terms and the Total Fluxes of ^{18}Ne
from ^{20}Ne Transport in Water

Depth (g/cm ²)	Total Flux and Fluxes of Different Collision Terms in (Ions/cm ²)				
	First Term	Second Term	Third Term	Fourth Term	Total Flux
5.000	1.48E-3	7.61E-5			1.56E-3
10.000	2.05E-3	7.61E-4			2.26E-3
15.000	2.12E-3	3.28E-4	Third and Fourth Collision Terms do not exist.		2.45E-3
20.000	1.96E-3	4.03E-4			2.36E-3
25.000	1.69E-3	4.35E-4			2.13E-3
30.000	1.41E-3	4.34E-4			1.84E-3
35.000	1.13E-3	4.08E-4			1.54E-3
40.000	8.97E-4	3.69E-4			1.27E-3
50.000	5.36E-4	3.23E-4			8.12E-4

Table 7
Successive Collision Terms and the Total Fluxes of ^{18}F
from ^{20}Ne Transport in Water

Depth (g/cm ²)	Total Flux and Fluxes of Different Collision Terms in (Ions/cm ²)				
	First Term	Second Term	Third Term	Fourth Term	Total Flux
5.000	6.74E-3	1.49E-4			6.89E-3
10.000	9.32E-3	4.12E-4			9.74E-3
15.000	9.67E-3	6.41E-4			1.03E-3
20.000	8.92E-3	7.88E-4	Third and Fourth Collision Terms do not exist.		9.71E-3
25.000	7.71E-3	8.51E-4			8.57E-3
30.000	6.40E-3	8.48E-4			7.25E-3
35.000	5.17E-3	7.99E-4			5.97E-3
40.000	4.08E-3	7.21E-4			4.80E-3
50.000	2.44E-3	5.39E-4			2.98E-3

Table 8
Successive Collision Terms and the Total Fluxes of ^{19}Ne
from ^{20}Ne Transport in Water

Depth (g/cm ²)	Total Flux and Fluxes of Different Collision Terms in (Ions/cm ²)				
	First Term	Second Term	Third Term	Fourth Term	Total Flux
5.000	7.95E-3				7.95E-3
10.000	1.09E-2				1.09E-2
15.000	1.13E-2				1.13E-2
20.000	1.04E-2	Second, Third, and Fourth Collision Terms do not exist.			1.04E-2
25.000	8.93E-3				8.93E-3
30.000	7.38E-3				7.38E-3
35.000	5.92E-3				5.92E-3
40.000	4.66E-3				4.66E-3
50.000	2.76E-4				2.76E-4

Table 9
Successive Collision Terms and the Total Fluxes of ^{19}F
from ^{20}Ne Transport in Water

Depth (g/cm ²)	Total Flux and Fluxes of Different Collision Terms in (Ions/cm ²)				
	First Term	Second Term	Third Term	Fourth Term	Total Flux
5.000	9.68E-3				9.68E-3
10.000	1.33E-2				1.33E-2
15.000	1.37E-2				1.37E-2
20.000	1.26E-2	Second, Third, and Fourth Collision Terms do not exist.			1.26E-2
25.000	1.09E-2				1.09E-2
30.000	8.99E-3				8.99E-3
35.000	7.22E-3				7.22E-3
40.000	5.68E-3				5.68E-3
50.000	3.36E-3				3.36E-3

Table 10
Successive Collision Terms and the Total Fluxes of ^{10}B
from ^{20}Ne Beam Transport in Water

Depth (g/cm ²)	Total Flux and Fluxes of Different Collision Terms in (Ions/cm ²)				
	First Term	Second Term	Third Term	Forth Term	Total Flux
5.000	3.24E-3	2.88E-4	9.99E-6	1.57E-7	3.54E-3
10.000	4.67E-3	8.30E-4	5.76E-5	1.87E-6	5.56E-3
20.000	4.87E-3	1.72E-3	2.39E-4	1.53E-5	6.86E-3
30.000	3.82E-3	2.03E-3	4.21E-4	4.04E-5	6.31E-3
40.000	2.67E-3	1.88E-3	5.19E-4	6.64E-5	5.14E-3
50.000	1.76E-3	1.54E-3	5.30E-4	8.45E-5	3.91E-3

Table 10
Successive Collision Terms and the Total Fluxes of ^{10}B
from ^{20}Ne Beam Transport in Water

Depth (g/cm ²)	Total Flux and Fluxes of Different Collision Terms in (Ions/cm ²)				
	First Term	Second Term	Third Term	Forth Term	Total Flux
5.000	3.24E-3	2.88E-4	9.99E-6	1.57E-7	3.54E-3
10.000	4.67E-3	8.30E-4	5.76E-5	1.87E-6	5.56E-3
20.000	4.87E-3	1.72E-3	2.39E-4	1.53E-5	6.86E-3
30.000	3.82E-3	2.03E-3	4.21E-4	4.04E-5	6.31E-3
40.000	2.67E-3	1.88E-3	5.19E-4	6.64E-5	5.14E-3
50.000	1.76E-3	1.54E-3	5.30E-4	8.45E-5	3.91E-3

Table 11
Successive Collision Terms and the Total Fluxes of ^{14}Ne
from ^{20}Ne Beam Transport in Water

Depth (g/cm ²)	Total Flux and Fluxes of Different Collision Terms in (Ions/cm ²)				
	First Term	Second Term	Third Term	Forth Term	Total Flux
5.000	5.14E-3	3.55E-4	6.52E-6	4.47E-8	5.49E-3
10.000	7.25E-3	1.00E-3	3.67E-5	5.73E-7	8.28E-3
20.000	7.21E-3	1.99E-3	1.46E-4	4.44E-6	9.35E-3
30.000	5.39E-3	2.24E-3	2.46E-4	1.12E-5	7.88E-3
40.000	3.58E-3	1.98E-3	2.90E-4	1.75E-5	5.87E-3
50.000	2.23E-3	1.54E-3	2.82E-4	2.13E-5	4.08E-3

Table 12
Successive Collision Terms and the Total Fluxes of ^7Li
from ^{20}Ne Beam Transport in Water

Depth (g/cm ²)	Total Flux and Fluxes of Different Collision Terms in (Ions/cm ²)				
	First Term	Second Term	Third Term	Forth Term	Total Flux
5.000	4.59E-3	3.75E-4	1.34E-5	2.26E-7	4.97E-3
10.000	6.75E-3	1.09E-3	7.81E-5	2.71E-6	7.93E-3
20.000	7.35E-3	2.35E-3	3.33E-4	2.32E-5	10.05E-3
30.000	6.03E-3	2.85E-3	6.02E-4	6.27E-5	9.54E-3
40.000	4.43E-3	2.74E-3	7.66E-4	1.06E-4	8.04E-3
50.000	3.06E-3	2.32E-3	8.07E-4	1.39E-4	6.33E-3

Table 13
Successive Collision Terms and the Total Fluxes of ^{12}C
from ^{20}Ne Beam Transport in Water.

Depth (g/cm ²)	Total Flux and Fluxes of Different Collision Terms in (Ions/cm ²)				
	First Term	Second Term	Third Term	Forth Term	Total Flux
5.000	6.44E-3	5.25E-4	1.26E-5	1.37E-7	6.97E-3
10.000	9.18E-3	1.49E-3	7.18E-5	1.53E-6	10.74E-3
20.000	9.34E-3	3.04E-3	2.91E-4	1.24E-6	12.66E-3
30.000	7.14E-3	3.47E-3	4.98E-4	3.18E-5	11.14E-3
40.000	4.88E-3	3.13E-3	5.98E-4	5.09E-5	8.66E-3
50.000	3.11E-3	2.49E-3	5.93E-4	6.29E-5	6.26E-3

Table 14
 Successive Collision Terms and the Total Fluxes of ^{55}Mn
 from ^{56}Fe Beam Transport in Water

Depth (g/cm ²)	Total Flux and Fluxes of Different Collision Terms in (Ions/cm ²)				
	First Term	Second Term	Third Term	Fourth Term	Total Flux
5.000	9.48E-2				9.48E-2
10.000	1.02E-2				1.02E-2
15.000	8.27E-3	Second, Third, and Fourth Collision Terms do not exist.			8.27E-3
20.000	5.94E-3				5.94E-3
25.000	4.00E-3				4.00E-3
30.000	2.59E-3				2.59E-3
35.000	1.63E-3				1.63E-3
40.000	1.00E-3				1.00E-3
50.000	3.64E-4				3.64E-4

Table 15
Successive Collision Terms and the Total Fluxes of ^{54}Mn from ^{56}Fe
Transport in Water

Depth (g/cm ²)	Total Flux and Fluxes of Different Collision Terms in (Ions/cm ²)				
	First Term	Second Term	Third Term	Fourth Term	Total Flux
5.000	1.04E-2	2.96E-4			1.07E-2
10.000	1.13E-2	6.41E-4			1.19E-2
15.000	9.15E-3	7.78E-4			9.93E-3
20.000	6.59E-3	7.49E-4	Third and Fourth Collision Terms do not exist.		7.35E-3
25.000	4.46E-3	6.33E-4			5.09E-3
30.000	2.89E-3	4.93E-4			3.38E-3
35.000	1.82E-3	3.63E-4			2.19E-3
40.000	1.13E-3	2.56E-4			1.38E-3
50.000	4.12E-4	1.17E-4			5.29E-4

Table 16
Successive Collision Terms and the Total Fluxes of ^{52}V
from ^{56}Fe Beam Transport in Water

Depth (g/cm ²)	Total Flux and Fluxes of Different Collision Terms in (Ions/cm ²)				
	First Term	Second Term	Third Term	Forth Term	Total Flux
5.000	1.16E-2	4.60E-4	6.88E-6	1.63E-7	1.21E-2
10.000	1.26E-2	1.00E-3	2.99E-5	2.84E-7	1.34E-2
15.000	1.03E-2	1.22E-3	5.49E-5	6.99E-7	1.16E-2
20.000	4.47E-3	1.18E-3	7.08E-5	1.29E-6	8.72E-3
25.000	5.06E-3	1.00E-3	7.52E-5	1.83E-6	6.16E-3
30.000	3.31E-3	7.85E-4	7.06E-5	1.98E-6	4.17E-3
35.000	2.10E-3	5.81E-4	6.10E-5	1.93E-6	2.75E-3
40.000	1.31E-3	4.12E-4	4.95E-5	1.84E-6	1.77E-3
50.000	4.83E-4	1.90E-4	2.89E-5	1.33E-6	7.04E-4

Table 17
 Successive Collision Terms and the Total Fluxes of ^{55}Fe
 from ^{56}Fe Transport in Water

Depth (g/cm ²)	Total Flux and Fluxes of Different Collision Terms in (Ions/cm ²)				
	First Term	Second Term	Third Term	Fourth Term	Total Flux
5.000	1.80E-2				1.80E-2
10.000	1.94E-2				1.94E-2
15.000	1.57E-2	Second, Third, and Fourth Collision Terms do not exist.			1.57E-2
20.000	1.13E-2				1.13E-2
25.000	7.61E-3				7.61E-3
30.000	4.92E-3				4.92E-3
35.000	3.09E-3				3.09E-3
40.000	1.91E-3				1.91E-3
50.000	6.92E-4				6.92E-4

Table 18

Normalized Contributions to the ^{52}V Fluxes from Successive
Collision Terms of ^{56}Fe Beam Transport in Water

Depth (g/cm ²)	Fluxes of Different Collision Terms in (Ions/cm ²)			
	First Term	Second Term	Third Term	Forth Term
5.000	1.00E 0	3.45E-2	5.92E-4	1.40E-5
10.000	1.00E 0	7.91E-2	2.37E-3	2.24E-5
15.000	1.00E 0	1.18E-1	5.33E-3	6.76E-5
20.000	1.00E 0	1.58E-1	9.48E-3	1.73E-4
25.000	1.00E 0	1.97E-1	1.48E-2	3.61E-4
30.000	1.00E 0	2.37E-1	2.13E-2	5.93E-4
35.000	1.00E 0	2.76E-1	2.90E-2	9.19E-4
40.000	1.00E 0	3.15E-1	3.79E-2	1.41E-3
50.000	1.00E 0	3.94E-1	5.91E-2	2.79E-3

Table 19
 Normalized Contributions to the ^{16}O Fluxes from Successive
 Collision Terms of ^{56}Fe Beam Transport in Water

Depth (g/cm ²)	Fluxes of Different Collision Terms in (Ions/cm ²)			
	First Term	Second Term	Third Term	Forth Term
5.000	1.00E 0	2.99E-1	4.77E-2	
10.000	1.00E 0	5.87E-1	1.86E-1	3.06E-2
15.000	1.00E 0	8.61E-1	4.09E-1	
20.000	1.00E 0	1.12E 0	7.08E-1	2.63E-1
25.000	1.00E 0	1.39E 0	1.07E 0	
30.000	1.00E 0	1.59E 0	1.49E 0	9.44E-1
35.000	1.00E 0	1.81E 0	1.96E 0	
40.000	1.00E 0	2.00E 0	2.46E 0	2.33E0
50.000	1.00E 0	2.36E 0	3.56E 0	4.72E 0

Table 20
Successive Collision Terms and the Total Fluxes of ^{28}Si from ^{56}Fe
Beam Transport in Water

Depth (g/cm ²)	Total Flux and Fluxes of Different Collision Terms in (Ions/cm ²)				
	First Term	Second Term	Third Term	Forth Term	Total Flux
5.000	1.34E-3	5.91E-4	8.49E-5	4.80E-6	2.03E-3
10.000	1.70E-3	1.49E-3	4.25E-4	5.14E-5	3.67E-3
20.000	1.37E-3	2.36E-3	1.34E-3	3.19E-4	5.39E-3
30.000	8.33E-4	2.12E-3	1.79E-3	6.39E-4	5.38E-3
40.000	4.55E-4	1.51E-3	1.69E-3	7.99E-4	4.45E-3
50.000	2.35E-4	9.54E-4	1.32E-3	7.75E-4	3.28E-3

Table 21
Successive Collision Terms and the Total Fluxes of ^{16}O
from ^{56}Fe Beam Transport in Water

Depth (g/cm ²)	Total Flux and Fluxes of Different Collision Terms in (Ions/cm ²)				
	First Term	Second Term	Third Term	Forth Term	Total Flux
5.000	2.28E-3	6.83E-4	1.08E-4		3.07E-3
10.000	2.84E-3	1.67E-3	5.31E-4	8.73E-5	5.13E-3
20.000	2.26E-3	2.53E-3	1.60E-3	5.96E-4	6.98E-3
30.000	1.38E-3	2.20E-3	2.06E-3	1.30E-3	6.94E-3
40.000	7.65E-4	1.53E-3	1.88E-3	1.78E-3	5.98E-3
50.000	4.06E-4	9.59E-4	1.45E-3	1.92E-3	4.73E-3

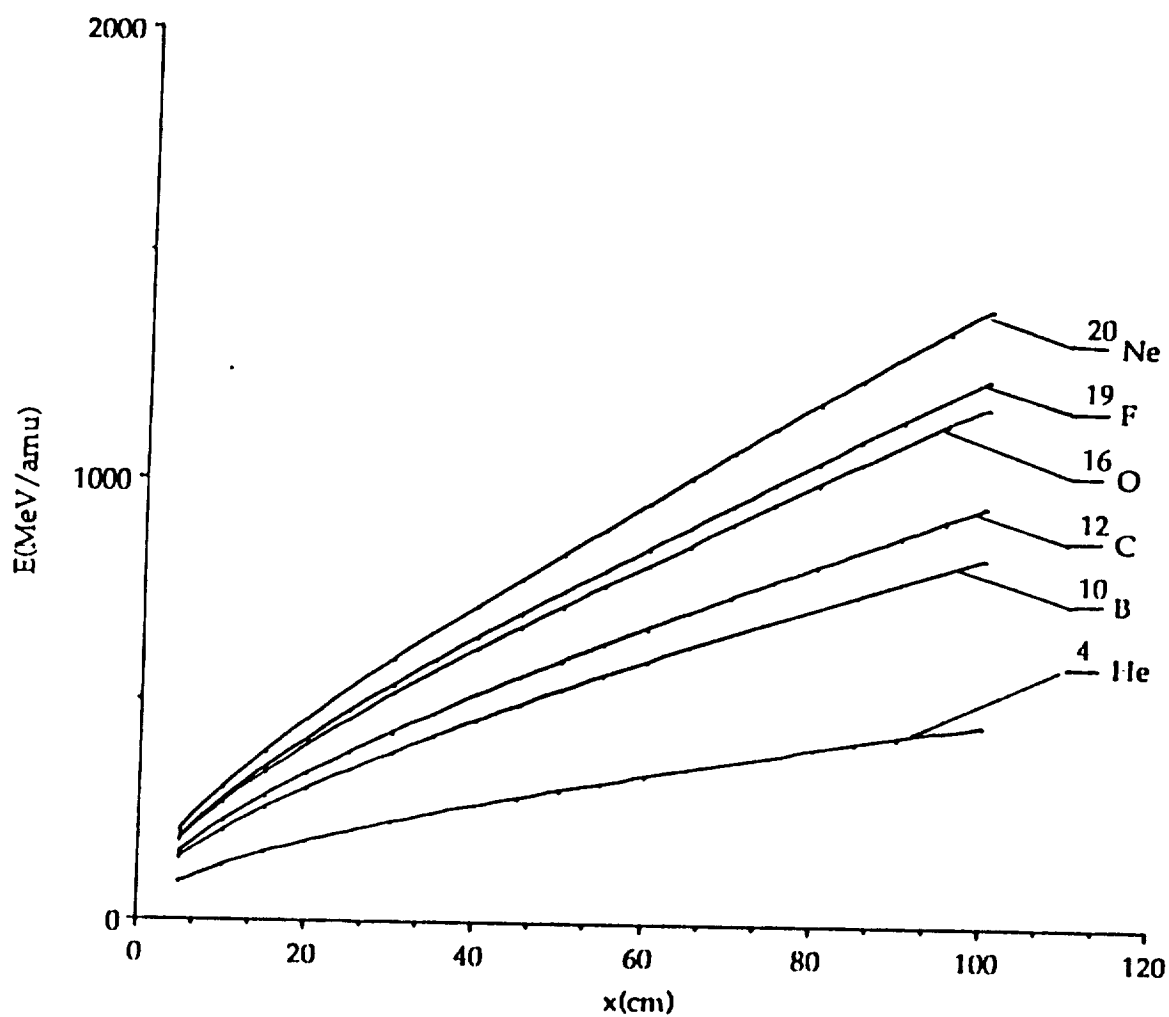


Figure 1. Range - Energy Relation for Ions Lighter than ^{20}Ne with the Least Initial Energy E to Pass x Thickness of Water

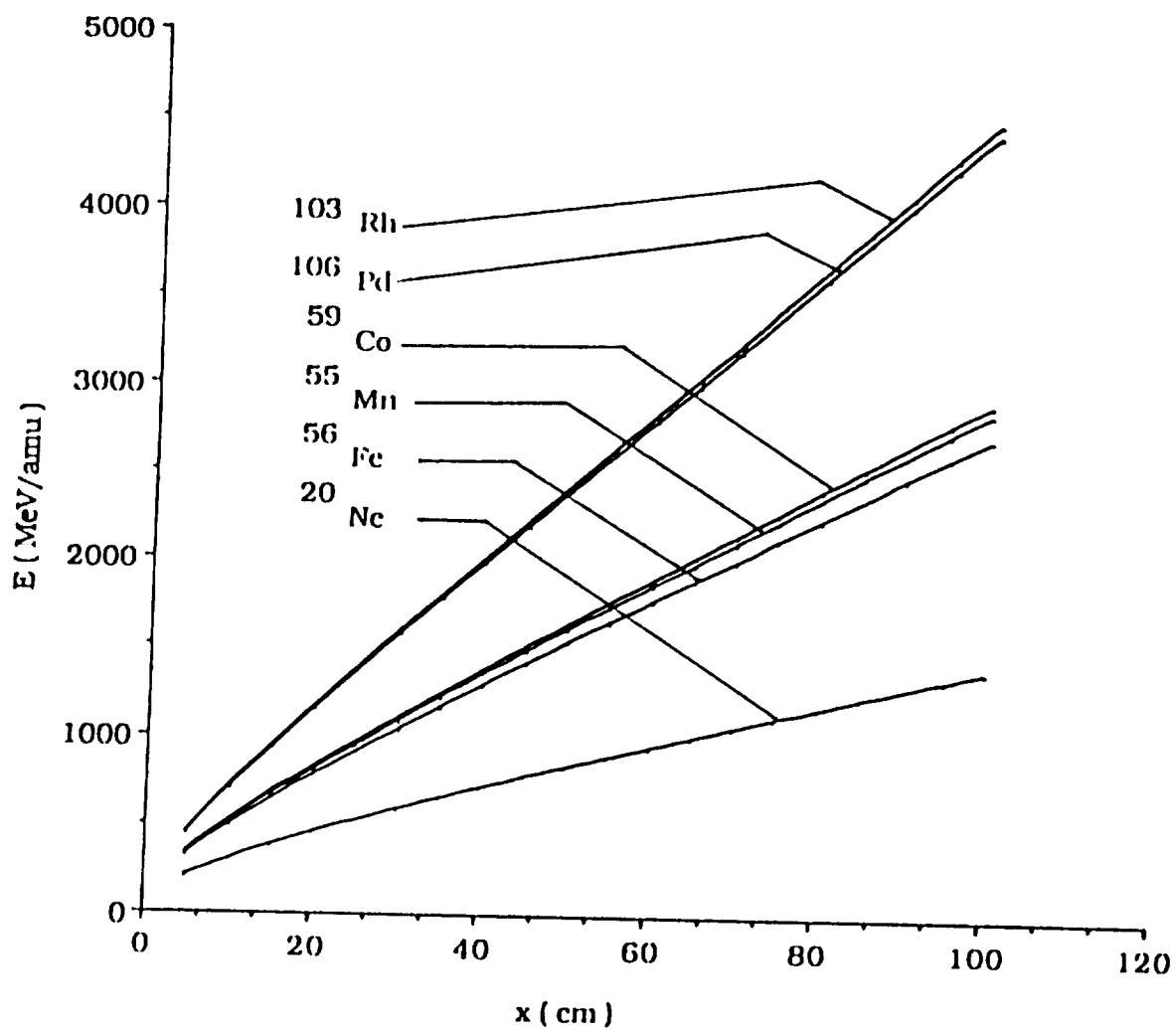


Figure 2. Range - Energy Relation for Ions Heavier than ^{20}Ne with the Least Initial Energy E to Pass x Thickness of Water

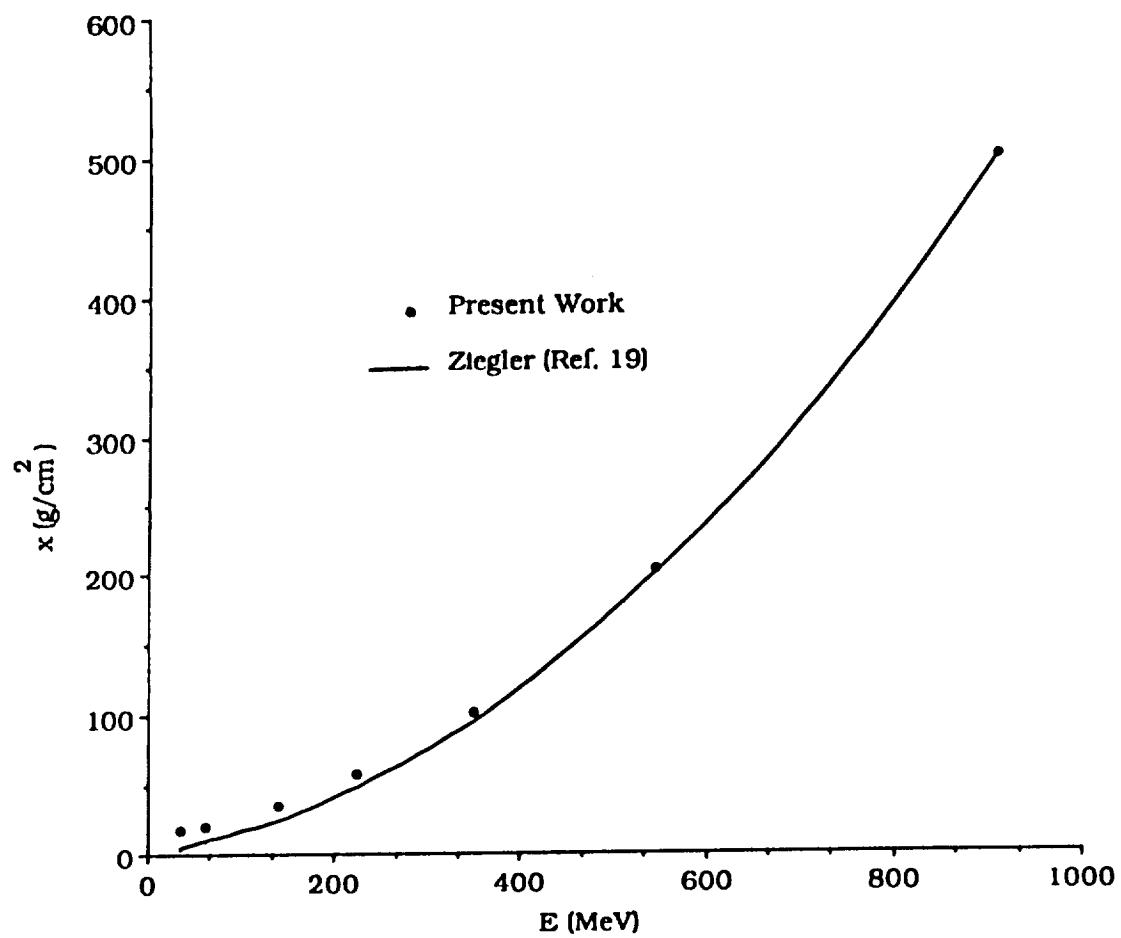


Figure 3. Range - Energy Relation of Incident ^{20}Ne Beam in ^{28}Si .

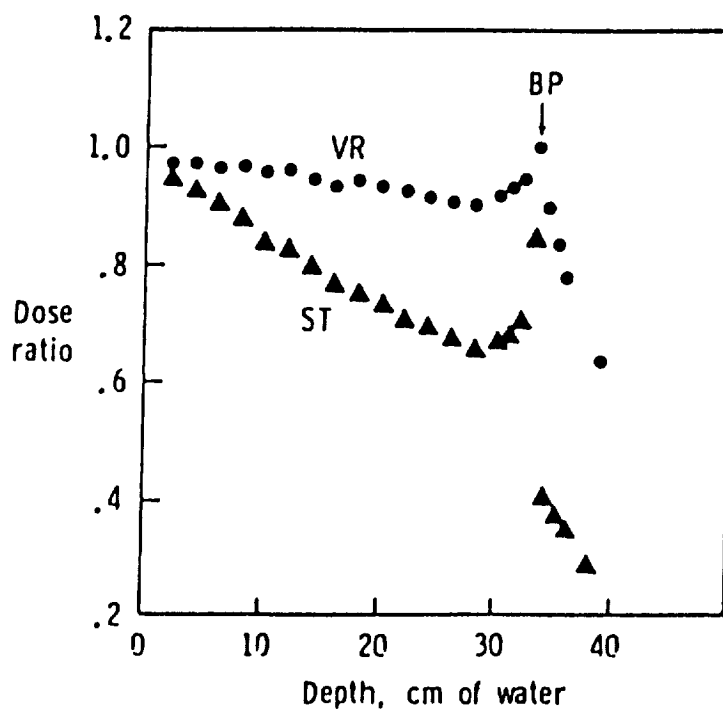


Figure 4. Ratio of Calculated to Experimental Doses, as a Function of Depth in Water, for a 670 MeV/nucleon ^{20}Ne Beam. The Calculation used Energy - Dependent Renormalized (VR) and Unrenormalized (ST) Silberberg - Tsao Fragmentation Parameters, and Energy - Independent Nuclear Absorption Cross Section. For Reference, the Bragg Peak Location is Labeled (BP).

Reprinted by Permission²⁰

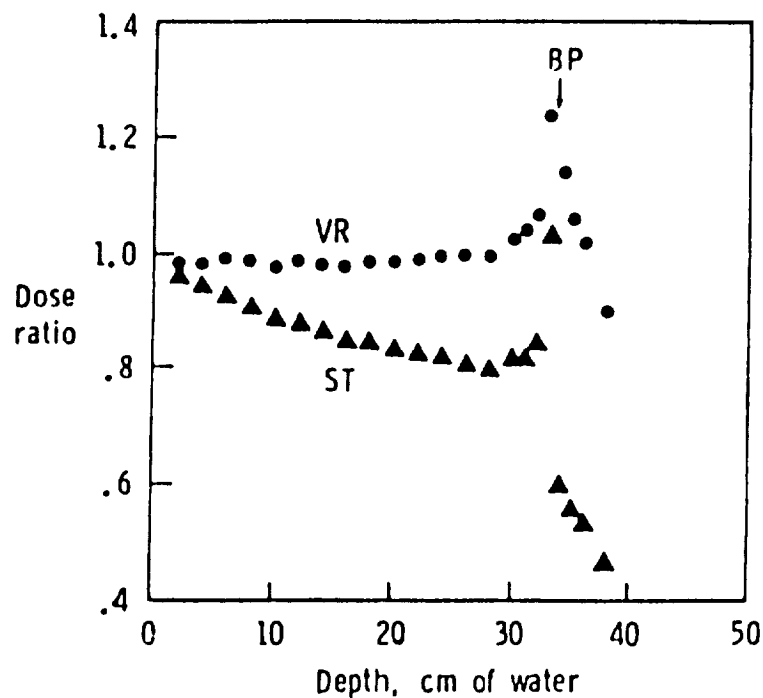


Figure 5. Ratio of Calculated to Experimental Doses, as a Function of Depth in Water, for a 670 MeV/nucleon ^{20}Ne Beam. The Calculation used Energy - Independent Renormalized (VR) and Unrenormalized (ST) Siberberg - Tsao Fragmentation Parameters. The Nuclear Absorption Cross Sections were Fully Energy - Dependent. For References, the Bragg Peak Location is Labeled (BP).

Reprinted by Permission²⁰

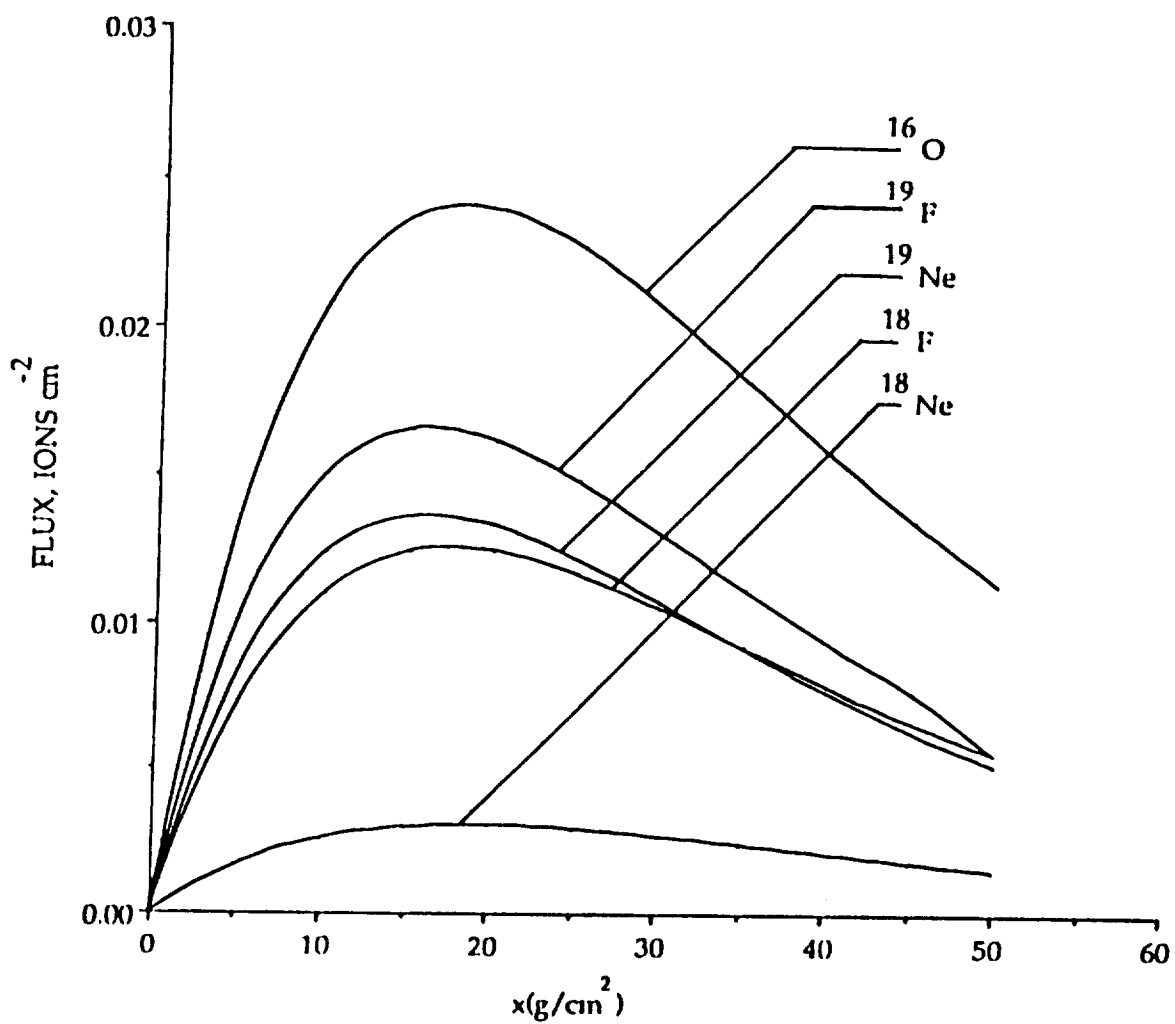


Figure 6. Ions Fragments Flux of Various Isotopes as a Function of Depth, from ^{20}Ne Beam Transport in Water

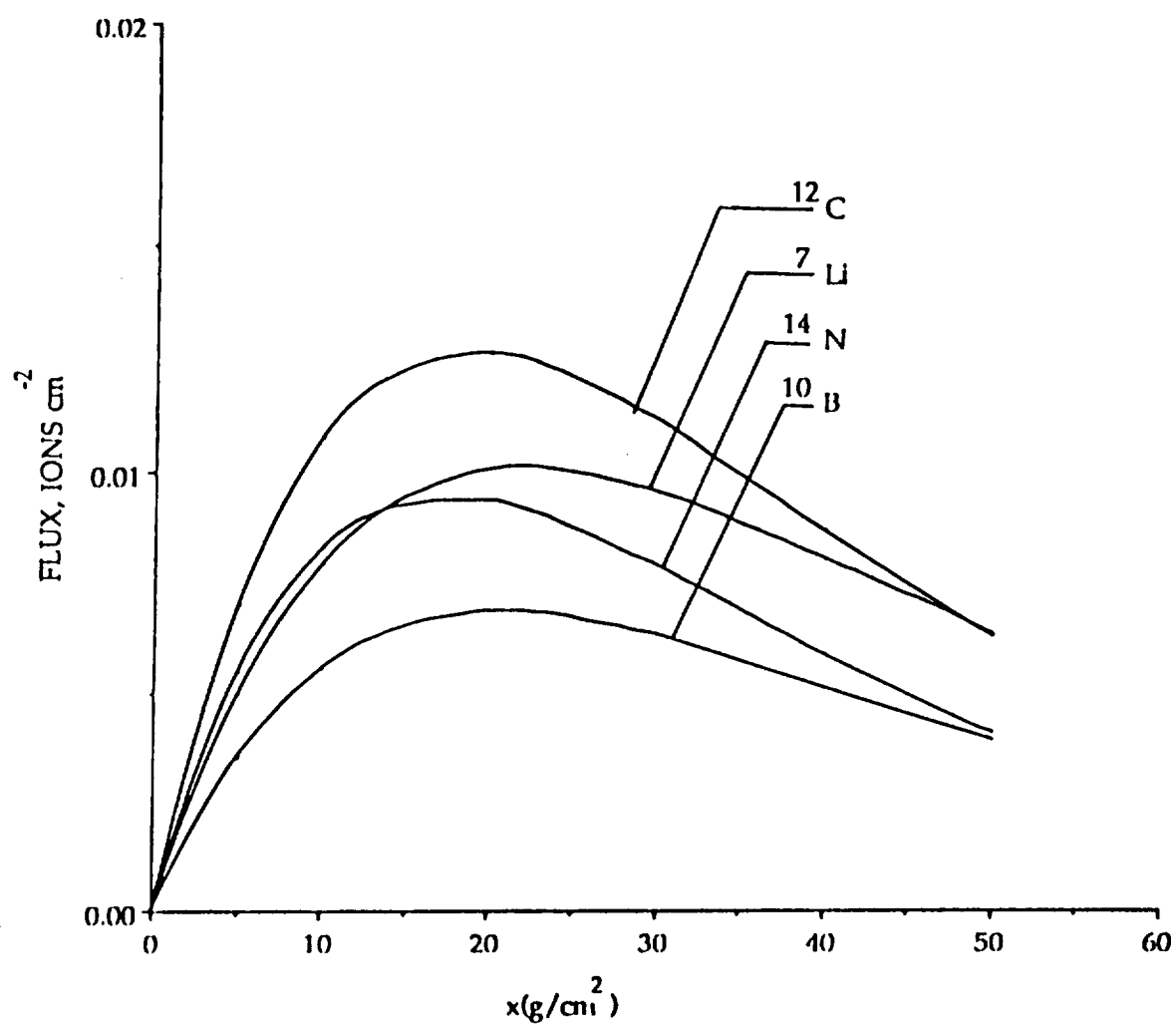


Figure 7. Flux of Some Light Ion Fragments as a Function of Depth, from ²⁰Ne Beam Transport in Water

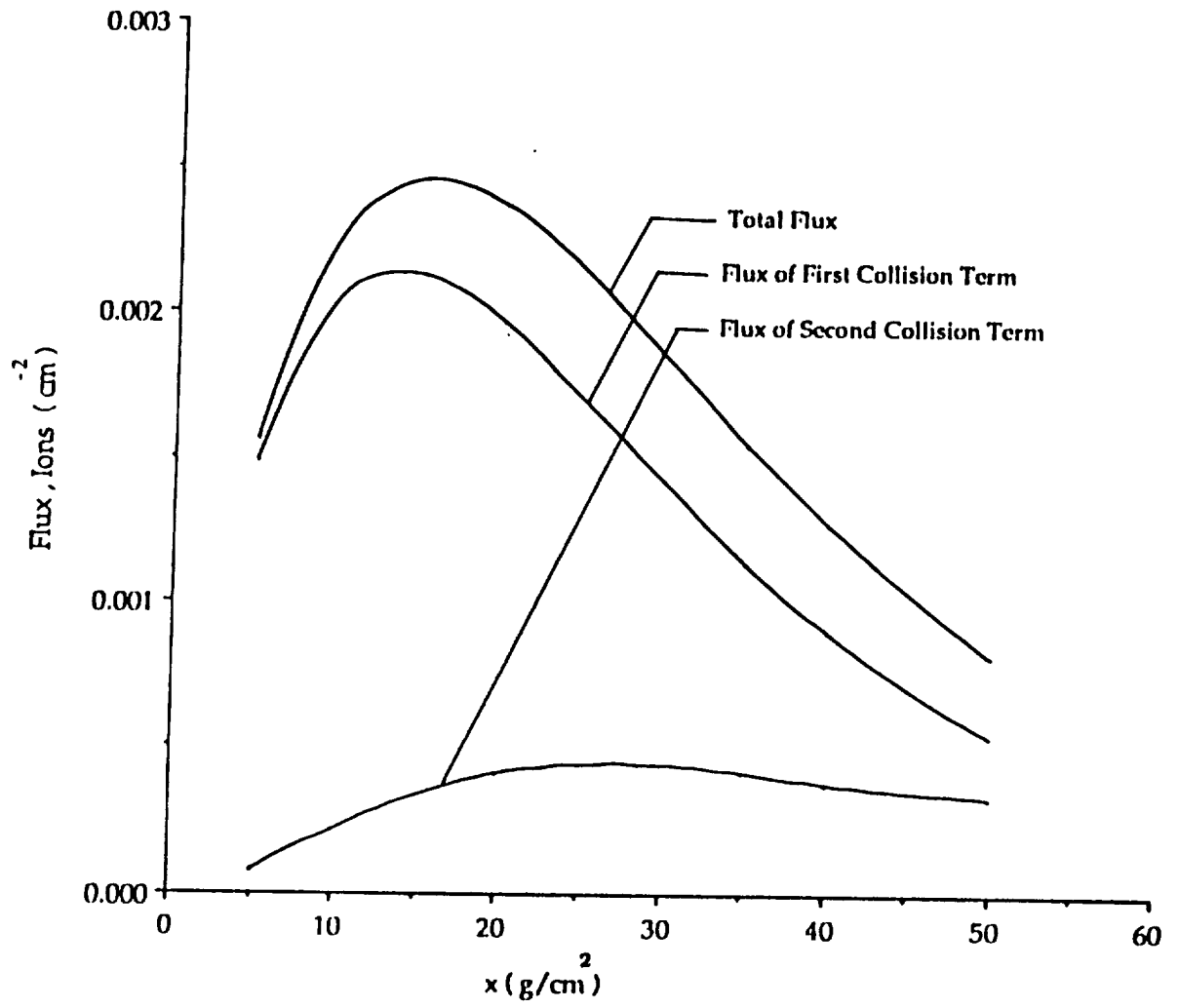


Figure 8. Successive Collision Terms and the Total Fluxes of ^{18}Ne from ^{20}Ne Transport in Water

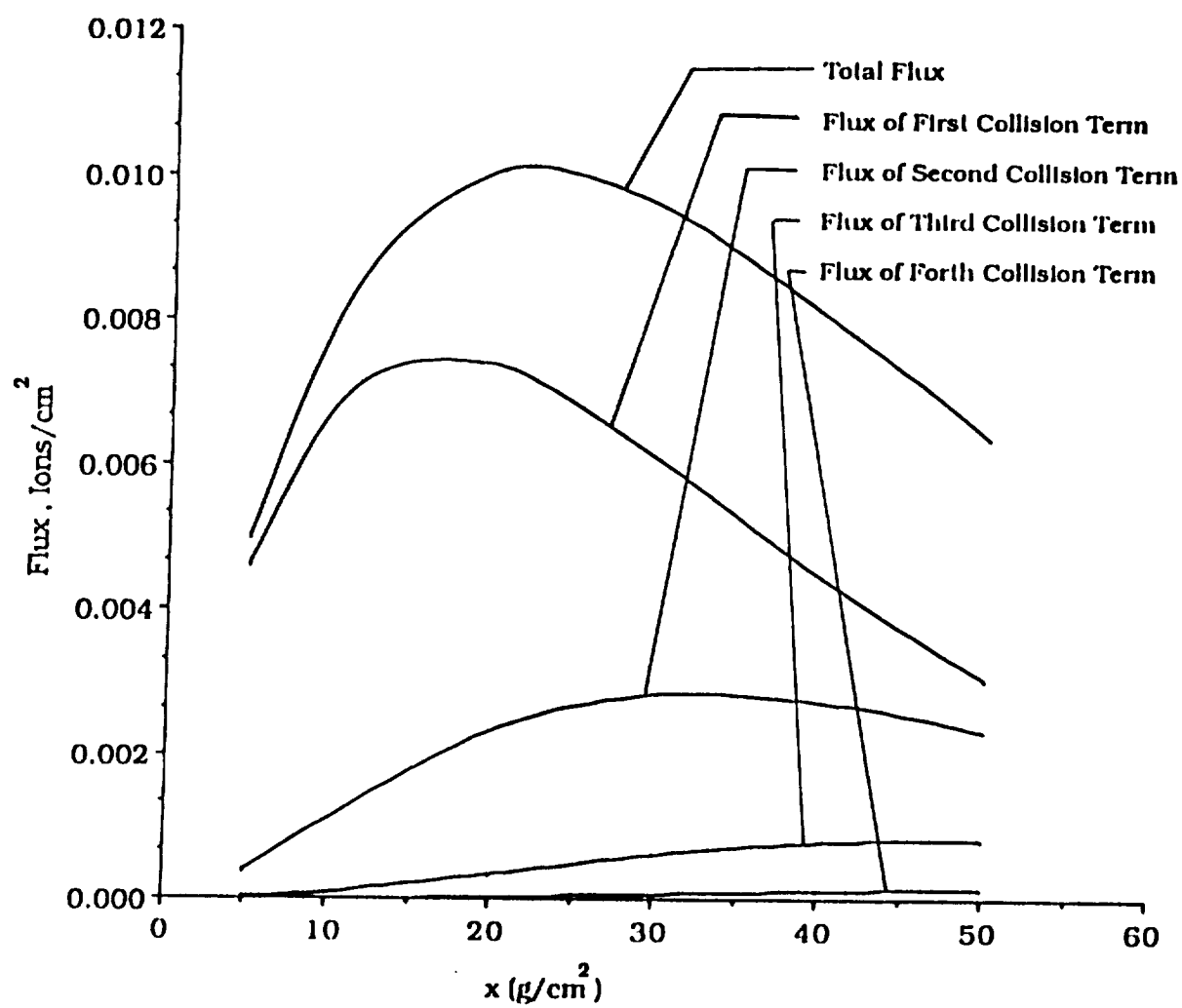


Figure 9. Successive Collision Terms and the Total Fluxes of ⁷Li from ²⁰Ne Beam Transport in Water

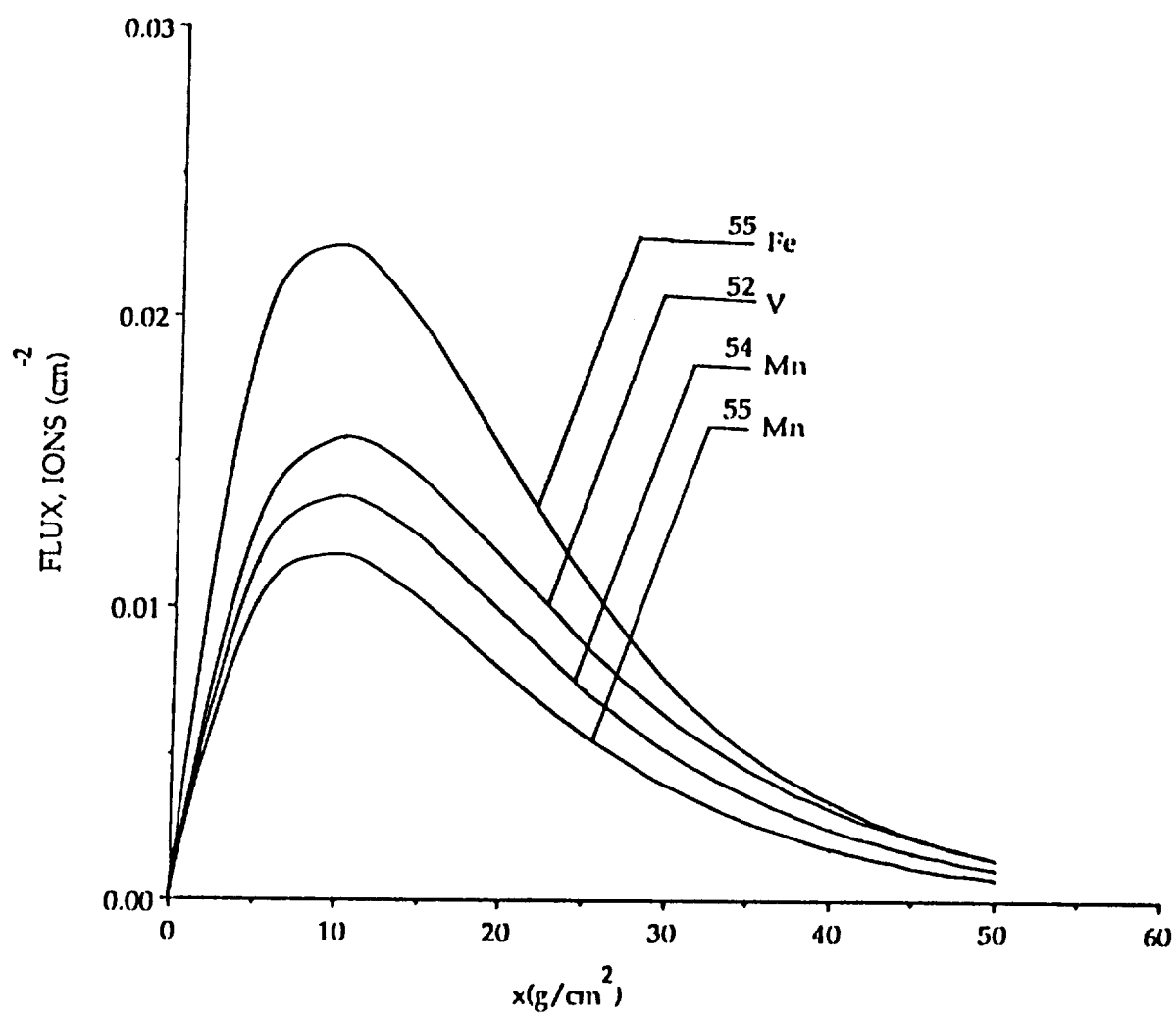


Figure 10. Ion Fragments of Various Isotopes as a Function of the Depth, from ^{56}Fe Beam Transport in Water

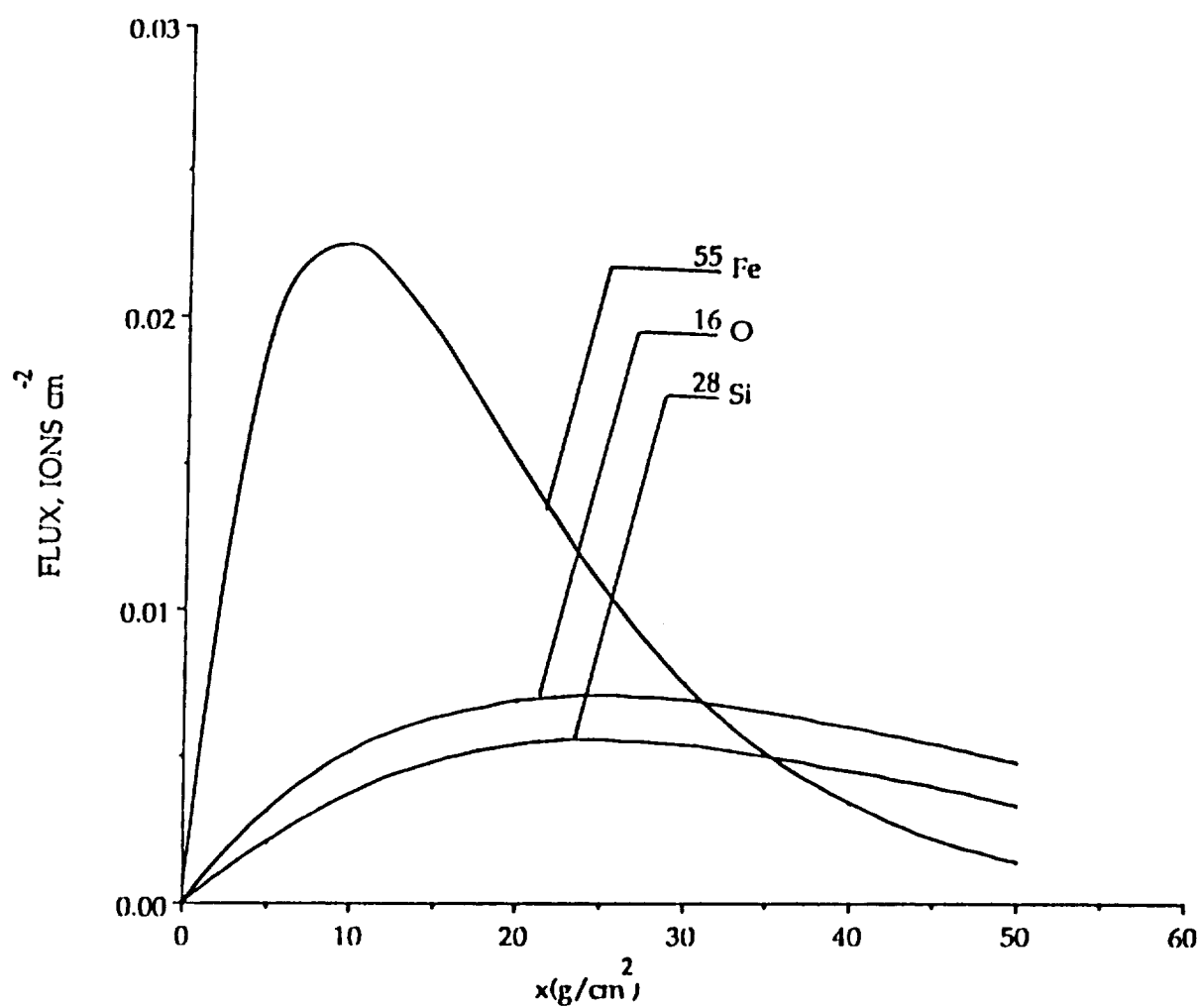


Figure 11. Total Flux of Light Ion Fragments Compared with ^{55}Fe Ion Fragments Flux, as a Function of Depth from ^{56}Fe Transport in Water

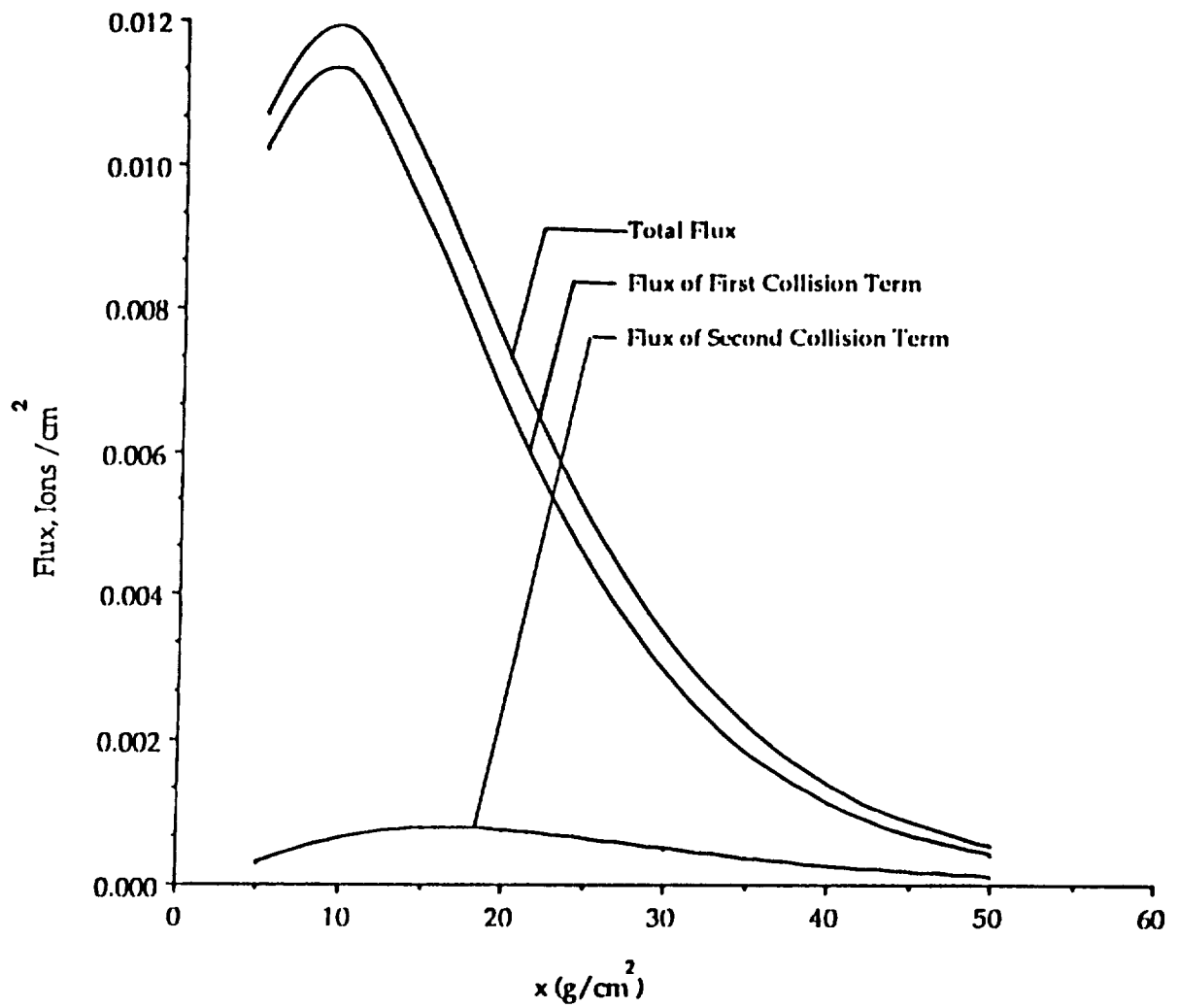


Figure 12. Successive Collision Terms and the Total Fluxes of ⁵²V from ⁵⁶Fe Transport in Water

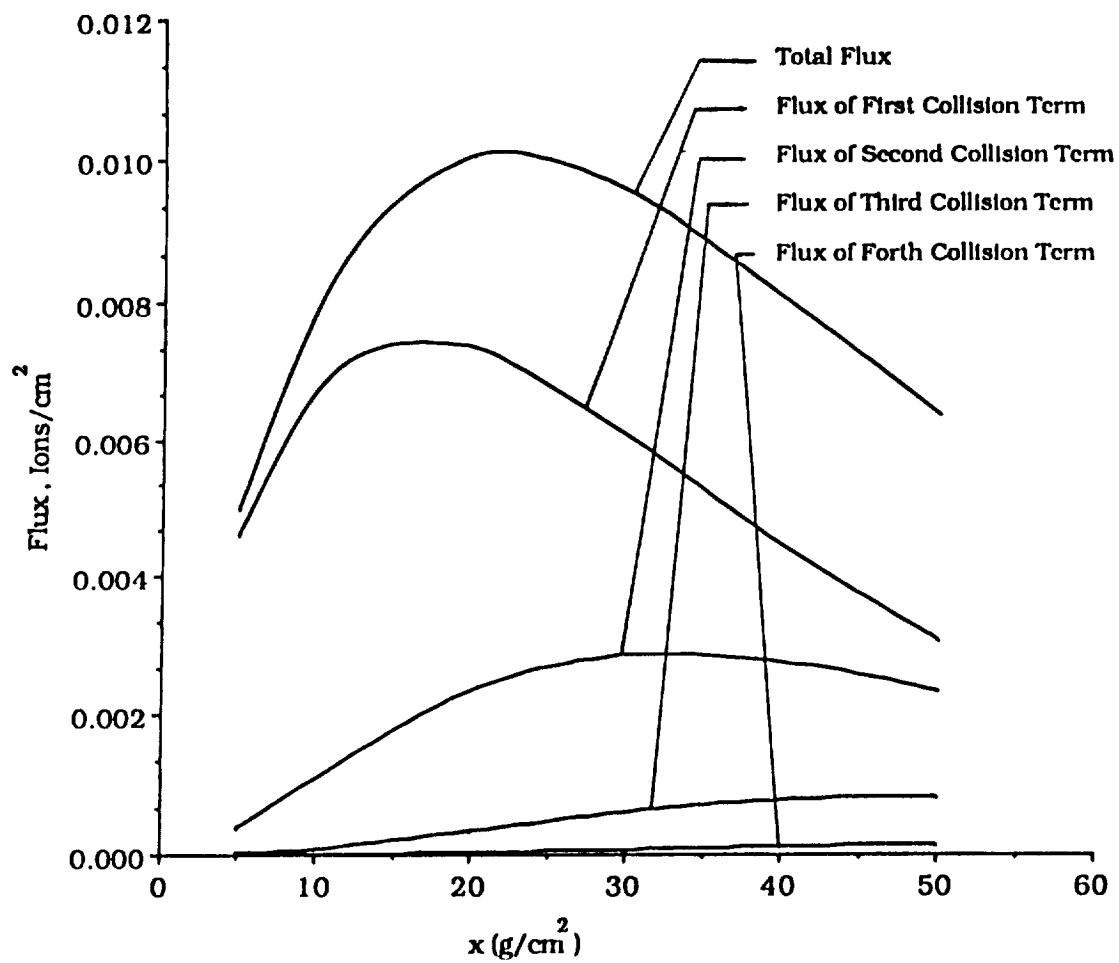


Figure 13. Successive Collision Terms and the Total Fluxes of ^{54}Mn from ^{56}Fe Beam Transport in Water.

REFERENCES

1. Townsend, L. W. and Wilson, J. W., Energy - Dependent Parameterization of Heavy-Ion Absorption Cross Section. *Rad. Res.* 106, 283-287 (1986).
2. Alsmiller, R. G., High-Energy Nucleon Transport and Space Vehicle Shielding. *Nuclear Science and Engineering.* 27, 158-189 (1967).
3. McDonald, F. B. and Fichtel, C. E., High Energy Particle and Quantum in Astrophysics. Massachusetts Institute of Technology Press, (1974).
4. Winckler, J. R., Primary Cosmic Rays. *Rad. Res.* 14, 521 (1956).
5. Matuusevich, E. S. and Tsypin, S. G., Radiation Shielding of Man in Space. *At. Energy. (USSR)* 15, 499 (1963).
6. McDonald, F. B., Solar Proton Manual. NASA-TR-169 (1963).
7. Curtis, S. B., Atwell, W., Beever, R., and Hardy, A., Radiation Environments and Absorbed Dose Estimation on Manned Space Mission. *Adv. Sp. Res.* 6, 269-274 (1986).
8. Curtis, S. B., Letaw, J. R., Galactic Cosmic Rays and Cell- Hit Frequencies Outside the Magnetosphere. Bristol England (1985).
9. Stassionopoulos, E. G. and Swendberg, C. E., Space Radiobiology Res. NASA, Washington, DC. X-600-87-3 (1987).
10. Gerald, J. H. and Gordon, L. B., Radiation Dosimetry. Academic Press Inc. Publishers. New York (1956).
11. Curtis, S. B., Track Structure in Biological Model. *Adv. Sp.6*, 179-185 (1986).
12. Schimmerling, W., Appleby, A., Todd, P. W., and Vosburg, K. G., Apparatus and Dosimetry of High-Energy Heavy Ion Beam Irradiation. *Rad. Res.* 65, 389-431 (1976).
13. Lyman, J. T., Heavy Charged Particle Beam Dosimetry Advances In Dosimetry of Fast Neutrons and Heavy Charged Particles for Therapy Applications. (conference proceeding), Vienna: IAEA-AG-371/13, 267-280 (1984).
14. Wilson, J. W. and Badavi, F. F., Method of Galactic Heavy Ion Transport. *Rad. Res.* 108, 231-237 (1986).

15. Wilson, J. W. and Townsend, L. W., A Benchmark for Galactic Cosmic Ray Transport Codes. *Rad. Res.* 114, 201 (1988).
16. Wilson, J. W., Townsend, L. W., and Badavi, F. F., Galactic HZE Propagation Through the Earth's Atmosphere. *Rad. Res.* 109, 173-183 (1987).
17. Wilson, J. W. and Townsend, L. W., A Benchmark for Galactic Cosmic Ray Transport Codes. *Rad. Res.* 114, 201 (1988).
18. Ziegler, J. F., The Stopping and Ranges of Ions in Matter. Vol.1-6, Pergamon Press (1977).
19. Littmark, U. and Ziegler, G. F., Handbook of Range Distributions for Energetic Ions in All Elements. Vol. 6, Pergamon Press (1977).
20. Townsend, L.W. and Wilson, J. W., An Evaluation of Energy Independent Heavy Ion Transport Coefficients Approximation. *Health Phys.*, Vol. 54, No. 4, 409-412 (1988).
21. Brandt, H. L. and Peter, B., The Heavy Nuclei of the Primary Cosmic Radiation. *Phys. Rev.* 77, 54-70 (1950).
22. Wilson, J. W., Townsend, L. W., and Badavi, F. F., A Semiempirical Nuclear Fragmentation Model. *Nucl. Instruments and Methods B*18, 225-231 (1987).
23. Ganapol, B. D., Townsend, L. W., and Wilson, J. W., Benchmark Solutions for the Galactic Ion Transport Equations: Energy and Spatially Dependent Problems. NASA TP -2878 (1989).
24. Wilson, J. W., Townsend, L. W., Bidasaria, H. B., Schimmerling, W. Wong, M., and Howard, J., ^{20}Ne Depth-Dose Relations in Water. *Health Phys.*, Vol. 46, No. 5, 1101-1111 (1984).

ABSTRACT

ONE DIMENSIONAL HEAVY ION BEAM TRANSPORT: ENERGY INDEPENDENT MODEL

**Student: Hamidullah Farhat
Date of Birth: January 05, 1955**

**Department: Physics
Advisor: Dr. W. W. Buck**

The present work, which is a step to better understand the nature of interaction of radiations (heavy ions) with matter, studies energy independent flux of heavy ion beam transport in one dimension (straight ahead approximation method). The transport of high energy heavy (HZE) ions through bulk materials that is studied here neglects energy dependence of the nuclear cross section. In the density range of 50 g/cm² for water a 833.43 MeV/nucleon neon beam and a 1579.68 MeV/nucleon iron beam represent the lower limit for high energy beams. The four term fluxes of secondary fragments which are given by an analytical solution of the energy independent transport equation, show that the fluxes of first and second collision terms are important, where the flux of third collision term is minor and the fluxes of fourth and higher order terms are negligible.